



**National
Oceanography Centre**
NATURAL ENVIRONMENT RESEARCH COUNCIL



EUMETSAT CALL-FOR-OFFER 205721

JASON-CS SAR MODE ERROR BUDGET STUDY

**REVIEW OF STATE OF KNOWLEDGE FOR SAR
ALTIMETRY OVER OCEAN**

CHRISTINE GOMMENGINGER¹

CRISTINA MARTIN-PUIG², LAIBA AMAROUCHE³

& R. KEITH RANEY⁴

¹NATIONAL OCEANOGRAPHY CENTRE – SOUTHAMPTON, UK;

²ISARDSAT, SPAIN; ³COLLECTE LOCALISATION SATELLITES, FRANCE;

⁴2KR-LLC, USA

EUMETSAT REFERENCE: EUM/RSP/REP/14/749304

21 NOVEMBER 2013

VERSION 2.2

© The Copyright of this document is the property of National Oceanography Centre (NOC). It is supplied on the express terms that it be treated as confidential, and may not be copied, or disclosed, to any third party, except as defined in the contract, or unless authorised by NOC in writing.

NATIONAL OCEANOGRAPHY CENTRE, SOUTHAMPTON

EUROPEAN WAY, SOUTHAMPTON SO14 3ZH



DOCUMENT SIGNATURE TABLE

	Name	Institution	Date
V1.0			
Prepared by	C. Gommenginger	NOC	04/04/2013
Authorized by	C. Gommenginger	NOC	04/04/2013
V1.1			
Prepared by	C. Gommenginger	NOC	12/06/2013
Authorized by	C. Gommenginger	NOC	12/06/2013
V2.2			
Prepared by	C. Martin-Puig	isardSAT	15/07/2013
	L. Amarouche	CLS	02/09/2013
	R. K. Raney	2kR, LLC	05/09/2013
	C. Gommenginger	NOC	21/11/2013
Authorized by	C. Gommenginger	NOC	21/11/2013



ISSUE RECORD

Issue No.	Issue Date	Sections affected	Relevant information
V1.0	04/04/2013	-	First draft
V1.1		All	Consolidated draft for input to Ocean SAR altimetry expert meeting at NOC, 26-27 June 2013
V2.1	15/07/2013	Table of Content only	New structure and additional technical content agreed within the writing team during discussions immediately after the SAR altimetry expert meeting at NOC, 26-27 June 2013.
V2.2	21/11/2013	All	Major revision of V1.1 to account for input from writing team



DISSEMINATION

To:	Copies	Means
Hans Bonekamp	1	Hans.Bonekamp@eumetsat.int
Cristina Martin-Puig	1	Cristina.Martin-Puig@isardsat.cat
R. Keith Raney	1	rkraney@gmail.com
Laiba Amarouche	1	lamarouche@cls.fr



EXECUTIVE SUMMARY

SAR altimetry over the ocean has attracted considerable attention in the past three years and remarkable progress has been made in a short space of time. Cryosat-2 is the first satellite to provide SAR altimeter data over the ocean, and the data helped to demonstrate the significant benefits of SAR mode for ocean altimetry compared to conventional low-resolution mode (LRM). This document provides an overview of the state of knowledge for SAR altimetry over the ocean based on research reported between 2010 and 2013.

There is increasing consensus between various independent investigation teams that SAR altimetry over the ocean leads to significant performance improvements when compared to even the best available conventional radar altimetry. The results are evident in reduced measurement noise, improved performance in coastal regions and improved spectral information content for Sea Level Anomaly at the ocean mesoscale. The convergence of results from different groups using different SAR waveform retracers indicates that there is now a high level of confidence in the ability to retrieve geophysical data from SAR mode altimetry over ocean.

Several issues particular to SAR altimetry remain open, specifically the sensitivity to platform mispointing, the lack of a sea state bias model in SAR mode, and the effects of swell and swell direction on SAR waveforms. It is noted that these issues disappear with SAR interleaved mode since the resulting SAR mode data can be transformed seamlessly into LRM data for self-calibration.

The document discusses differences between SAR closed-burst and SAR interleaved mode and the transformation of SAR data into pseudo-LRM waveforms. Closed-burst SAR used on CryoSat-2 and Sentinel-3 can be transformed into pseudo-LRM waveforms that look similar to LRM but are not statistically equivalent to real LRM data. Lack of equivalent P-LRM waveforms from closed burst SAR mode data precludes direct SAR/LRM cross-calibration. This fact jeopardizes the self-calibration potential of a closed burst SAR mode altimeter, and compromises attempts to relate - with sufficient confidence and precision - the closed-burst SAR sea level measurements to the existing sea level record. Adopting closed-burst SAR on Jason-CS would compromise the continuity of the high-precision sea level 20-year time series. In contrast, SAR interleaved would realize the theoretically optimal performance expected from a SAR mode altimeter, while ensuring continuity with conventional altimeters. This report explains that the SAR interleaved mode is essential since it is the only method that would assure continuity between the SAR mode aboard Jason-CS, and contemporaneous and prior conventional altimetric missions.

The main recommendations from the report are:

- Jason-CS should be implemented with the SAR Mode, which is the state-of-the art in radar altimetry, having been demonstrated in orbit with CryoSat-2, with significant benefits for many ocean applications.
- The Jason-CS SAR mode should be interleaved so that its products provide seamless continuity with the sea level measurement record established by prior altimeters in the TOPEX/Poseidon/Jason reference orbit, and so that its measurements satisfy its prime mission requirements for long-term continuity of sea level monitoring.



TABLE OF CONTENTS

DOCUMENT SIGNATURE TABLE.....	2
ISSUE RECORD	3
DISSEMINATION.....	4
EXECUTIVE SUMMARY	5
TABLE OF CONTENTS	6
1. INTRODUCTION AND SCOPE OF THIS DOCUMENT.....	8
2. CONTENT OF THIS DOCUMENT	9
3. HISTORICAL EVOLUTION OF SATELLITE ALTIMETRY MISSIONS.....	10
3.1. CONVENTIONAL ALTIMETRY	10
3.2. SAR ALTIMETRY.....	11
3.2.1. <i>Historical context</i>	11
3.2.2. <i>Cryosat-2</i>	12
4. LRM AND SAR MODES: CLOSED BURST VS INTERLEAVED OPERATION AND TRANSFORMATION TO PSEUDO-LRM	14
4.1. LRM AND SAR MODES: CLOSED BURST VS INTERLEAVED OPERATION	14
4.2. PSEUDO-LRM IN SAR CLOSED-BURST	16
5. ADVANCES WITH SAR ALTIMETRY OVER THE OCEAN	17
6. CONCLUSIONS.....	18
APPENDIX A. IMPROVED PERFORMANCE OF SAR MODE ALTIMETRY OVER OCEAN.....	20
A.1. REDUCED MEASUREMENT NOISE IN SAR MODE.....	20
A.1.1. <i>Cryosat-2 SAR with Cryosat-2 P-LRM</i>	20
A.1.2. <i>Cryosat-2 SAR versus Jason-2 LRM</i>	23
A.1.3. <i>Sub-cm range noise with SAR interleaved mode on Jason-CS</i>	24
A.2. GLOBAL COMPARISONS OF CRYOSAT-2 LRM, P-LRM AND SAR DATA.....	25
A.3. IMPROVED SEA SURFACE HEIGHT SPECTRA AT SHORT OCEAN WAVELENGTHS.....	29
A.4. IMPROVED ALTIMETER DATA QUALITY AND AVAILABILITY IN COASTAL REGIONS	31
A.5. VALIDATION OF SAR SWH AGAINST BUOYS.....	32
APPENDIX B. SAR ALTIMETER WAVEFORMS AND RETRACKING MODELS	35
B.1. NUMERICAL SAR WAVEFORM MODELS.....	37



B.2. SEMI-ANALYTICAL SAR WAVEFORM MODELS	37
B.3. FULLY-ANALYTICAL PHYSICALLY-BASED SAR WAVEFORM MODELS.....	37
B.4. EMPIRICAL SAR WAVEFORM MODELS.....	38
APPENDIX C. OPEN ISSUES.....	39
C.1. SENSITIVITY TO PLATFORM MISPOINTING	39
C.2. SSB IN SAR MODE.....	39
C.3. EFFECT OF SWELL AND SWELL DIRECTION ON SAR MODE WAVEFORMS.....	40
APPENDIX D: LRM AND SAR MODES: CLOSED BURST VS INTERLEAVED OPERATION	42
APPENDIX E. TRANSFORMATION OF SAR-MODE DATA INTO PSEUDO-LRM WAVEFORMS.....	46
E.1. REPLICATING LRM WAVEFORMS FROM SAR-MODE DATA	46
<i>E.1.1. Classical Conventional Brown-style Waveform</i>	<i>46</i>
E.2 RDSAR OPTIONS (FIVE CASES)	48
<i>E.2.1. Interleaved paradigm (Cases 1 and 2).....</i>	<i>48</i>
<i>E.2.2. CryoSat-2, closed-burst paradigm (Cases 3 – 5).....</i>	<i>49</i>
<i>E.2.3. The effects of SWH on Pseudo-LRM waveforms.....</i>	<i>50</i>
9. LIST OF ACRONYMS	53
10. REFERENCES.....	54



1. INTRODUCTION AND SCOPE OF THIS DOCUMENT

This document presents a review of the current state of knowledge for SAR altimetry over the ocean. The review is based on scientific results available in the public domain in the form of published papers, open-access reports and presentations at conferences between 2010 and 2013. The most recent results reported here are based on oral contributions made at the Ocean Surface Topography Science Team 2012 meeting (September 2012, Venice), the Cryosat'2013 User meeting (March 2013, Dresden) and the Ocean SAR altimetry expert group meeting at National Oceanography Centre (June 2013, Southampton, UK).

This report is the main deliverable of the Jason-CS SAR Mode error budget study awarded in response to the EUMETSAT Call-for-Offer 205721.

The document was developed as follows:

- V1.0 represents the first draft prepared by NOC.
- V1.1 is comprised of a consolidated draft, prepared by NOC, taking into account comments on V1.0 by EUMETSAT. The consolidated draft was distributed to other members of the writing team (Cristina Martin-Puig, Laiba Amarouche and R. Keith Raney) prior to the Ocean SAR altimetry expert group meeting at NOC on 26-27 June 2013.
- V2.0 represents the draft final report, prepared by NOC and other members of the writing team, after the Ocean SAR altimetry expert group meeting at NOC on 26-27 June 2013.
- V2.2 includes amendments, additions, and other editorial and substantive changes to the structure of the prior versions.

The review provides an overview of recent research activities and findings relevant to SAR altimetry over ocean. Selected major technical themes are offered as Appendices. The main objective is to summarise the key facts relevant to Jason-CS arising from recent experience with SAR altimetry over the ocean, to help inform recommendations for the future Jason-CS mission.

The high-level mission objectives of Jason-CS are to serve as a low noise reference mission for sea level monitoring, to assure compatibility with contemporaneous measurements from other altimeters, and to sustain continuity with over 20 years of high accuracy and precision measurements from the reference missions (TOPEX/Poseidon and Jason series). Those objectives demand state-of-the-art measurement performance.

This report shows that SAR mode provides important advantages in terms of range noise reduction, sampling of the ocean mesoscale and performance near land compared to conventional altimeters, but that continuity with the reference missions can only be achieved if the proposed SAR interleaved mode is implemented.



2. CONTENT OF THIS DOCUMENT

The document is organised into a main report with all technical material provided in Appendices.

Following this Section 2, the main body of the report consists of:

- Section 3: a brief summary of the historical evolution of ocean-viewing satellite-based radar altimetry, noting key technical milestones, leading up to SAR altimetry on Cryosat-2.
- Section 4: a top-level exploration of conventional (LRM) radar altimetry, introducing the two operational forms of the SAR mode (“Closed-burst” versus “Interleaved”), and exploring the transformation of SAR mode data into LRM waveforms
- Section 5: a summary of the advances with SAR altimetry over the ocean.
- Section 6: a conclusion section outlining the main findings of the review, with recommendations in support of SAR interleaved mode on Jason-CS.

Following the main body of the report, there are five technical appendices, each dealing with a particular theme:

- Appendix A presents the evidence that shows SAR-mode measurements to be much improved relative to those obtained in LRM over the ocean.
- Appendix B describes the principal characteristics of SAR-mode waveforms, noting especially their significant differences with respect to conventional radar altimeter waveforms, and presents the different SAR waveform models that exist to retrieve ocean geophysical parameters from SAR-mode data
- Appendix C cites three open issues with SAR altimetry that are still under investigation: the sensitivity of SAR measurements to platform mispointing; the lack of a Sea State Bias (SSB) model in SAR mode; the distortion of SAR waveforms in the presence of long swell waves. It is noted that these do not pose a serious challenge to SAR mode altimetry if SAR interleaved mode is adopted for Jason-CS.
- Appendix D presents a detailed discussion of the SAR closed-burst v interleaved modes of operation.
- Appendix E reviews progress and results of emulating conventional (LRM) waveforms from SAR-mode data, concluding that closed burst SAR data are not sufficient to support the main objectives of the Jason-CS mission.



3. HISTORICAL EVOLUTION OF SATELLITE ALTIMETRY MISSIONS

This section provides an historical context of ocean viewing satellite-based radar altimetry. The SAR-mode is the current state-of-the-art, having been demonstrated for the first time from an Earth-orbiting satellite on CryoSat-2, an ice-oriented mission. Despite its apparent novelty, in fact the technique rests on decades of excellent solid precedent. It is notable that SAR-mode altimetry is the first paradigm-shifting technical advance in radar altimetry since full de-ramp pulse modulation was introduced nearly 40 years ago (MacArthur, 1976).

3.1. CONVENTIONAL ALTIMETRY

All space-based Earth-observing radar altimeters prior to CryoSat-2 were conventional, in the sense that they transmitted pulses, whose reflections from the surface were processed on a pulse-by-pulse basis, incoherently. The main steps in their processing consisted of pulse compression, square-law detection, and summation of several similar post-detection waveforms. This report refers to that generic algorithm as “incoherent”, since no advantage is taken to extract information from the relative phase between subsequent reflections.

The pioneer of this family of radar altimeters was aboard Skylab (1973)¹. The S-193 altimeter aboard Skylab (Hayne, 1980) was followed by GEOS-C (1975) and Seasat (1978). The altimeter aboard Seasat introduced several significant design innovations that became standard for all subsequent altimeters (MacArthur, 1976, MacArthur *et al.*, 1989). GEOSAT (1985), TOPEX/Poseidon (1992), ERS-1 and ERS-2 (1991, 1995), GFO (1998), ENVISAT (2002) and the Jason-1 and Jason-2 family (2001, 2009) complete the list of conventional oceanographic radar altimeter missions. These altimeters operate in Ku-band (~13 GHz, about 2.2 cm wavelength), and, except for S-193 on Skylab, their footprints were pulse-limited (Raney, 2005, 2008).

In February 2013, AltiKa was launched on the French/Indian SARAL mission. Although AltiKa features several interesting technical innovations, it operates at a different frequency (Ka-band, 35.75 GHz) and a non T/P reference orbit, and is therefore not relevant to the Jason-CS mission.

The accomplishments of conventional radar altimetric missions have been reported in many thousands of professional papers (Fu & Cazenave, 2001). The heritage most relevant to the sea-level monitoring objectives of Jason-CS mission comes from the TOPEX/Poseidon and subsequent Jason series. The T/P-Jason series is unique, in that they are the only altimeters to continuously occupy the so-called reference orbit. One noteworthy achievement of the T/P-Jason series is the measurement of the global sea level trend to an accuracy of the order of one millimetre per year. TOPEX/Poseidon and its Jason successors are recognized as the “gold standard” for sea level monitoring with space-based oceanographic radar altimetry. Jason-CS is required to be as good, or better, than its predecessors.

¹ The launch dates of these missions are noted in parentheses.

² Further discussion of the Cryosat-2 operating modes is found in Section 4.

³ Subject to the inherent limitations imposed by the closed burst SAR mode used by CryoSat-2

⁴ <http://www.satoc.eu/projects/samosa/>

State of Knowledge for SAR altimetry over ocean

21/11/2013

⁵ Hertz is the standard unit name for “cycles per second”, abbreviated “Hz”.

⁶ The requirement to avoid Doppler ambiguities would apply if the radar were side-looking as is the



3.2. SAR ALTIMETRY

SAR altimetry measurements over the ocean provide significant advantages over conventional altimetry. The technical evidence to support this claim is presented in Appendix A. The three main advantages of SAR altimetry are:

- the greater pulse-to-pulse averaging leads to better precision (reduced noise) in range and other measurements (Section A.1)
- a much smaller along-track footprint (resolution), leading to the ability to resolve shorter-scale ocean features (mesoscale; Section A.3) and improved performance near land (Section A.4)
- the along-track resolution is constant, and does not increase with increasing significant wave heights (as in the case of conventional altimetry)

Thus, in Cryosat-2 SAR mode, the nominal along-track resolution is about 300m, regardless of significant wave height. In contrast, conventional altimeters have footprints of the order of 1.7 km over a quasi-flat sea, growing to about 3 km for a typical value of significant wave height of 2 m.

3.2.1. HISTORICAL CONTEXT

The first fully-documented application of Synthetic Aperture Radar (SAR) to altimeter design and processing was the Magellan instrument aboard NASA's mission to Venus Ford & Pettengill, 1992. At about the same time, Barbarossa & Picardi (1990) described a radar altimeter based on SAR principles, while Hartl & Kim (1990) described the application of SAR to altimetry, with the addition of interferometry for topography purposes.

In the mid-1990s, Dr. R. Keith Raney from John Hopkins University Applied Physics Laboratory (JHU-APL) proposed the Delay/Doppler radar altimeter concept Raney, 1998, also known as the SAR altimeter (or SAR-mode altimeter). The first SAR altimeter instrument was designed, built and demonstrated by JHU-APL as an airborne prototype. The Delay/Doppler Phase-Monopulse altimeter (D2P) is an airborne SAR mode altimeter paired with a cross-track interferometer, which was subsequently deployed over Greenland and the Arctic in support of pre-Cryosat field campaigns sponsored by ESA (Raney & Leuschen, 2002).

Results from the D2P instrument were consistent with the performance predicted, especially the small along-track footprint, and the increased precision of surface height measurement (Raney & Jensen, 2000). At the same time, ESA initiated hardware and software simulation studies for a high-resolution radar altimeter combining, like the D2P, SAR and interferometry. Encouraged by the results, CryoSat-1 "phase A" feasibility studies commenced in 2000. Between 2002 and 2005, airborne campaigns with the European Airborne SAR/Interferometric Radar Altimeter System (ASIRAS) provided further evidence and validating the design of the CryoSat-1 Synthetic Interferometric Radar Altimeter (SIRAL) instrument.

Unfortunately, CryoSat-1 was lost on launch in October 2005 due to a failure of the second stage to separate from the Eurokot launcher. Its replacement, Cryosat-2, was approved for full funding only a few months after the loss of CryoSat-1, and was successfully launched in April 2010.

3.2.2. CRYOSAT-2

CryoSat-2 is the ESA “ice mission” and its primary scientific objective is to reduce uncertainties in the knowledge of sea-ice thickness to improve the understanding of the mass balance of the major land ice fields. Cryosat-2 has three mutually exclusive operating modes:

- Low Resolution Mode (LRM), equivalent to a conventional ocean altimeter
- SAR mode, mainly over sea ice but also over some ocean, coastal and inland water regions
- SARIn mode, used mainly over sloping ice sheets².

The data acquired by Cryosat-2 in SAR mode over water surfaces are the first spaceborne SAR altimeter data available to assess the capabilities of SAR-mode altimetry for oceanography and hydrology.

Cryosat-2 uses a mode mask to determine regions in which each mode operates (Figure 1).

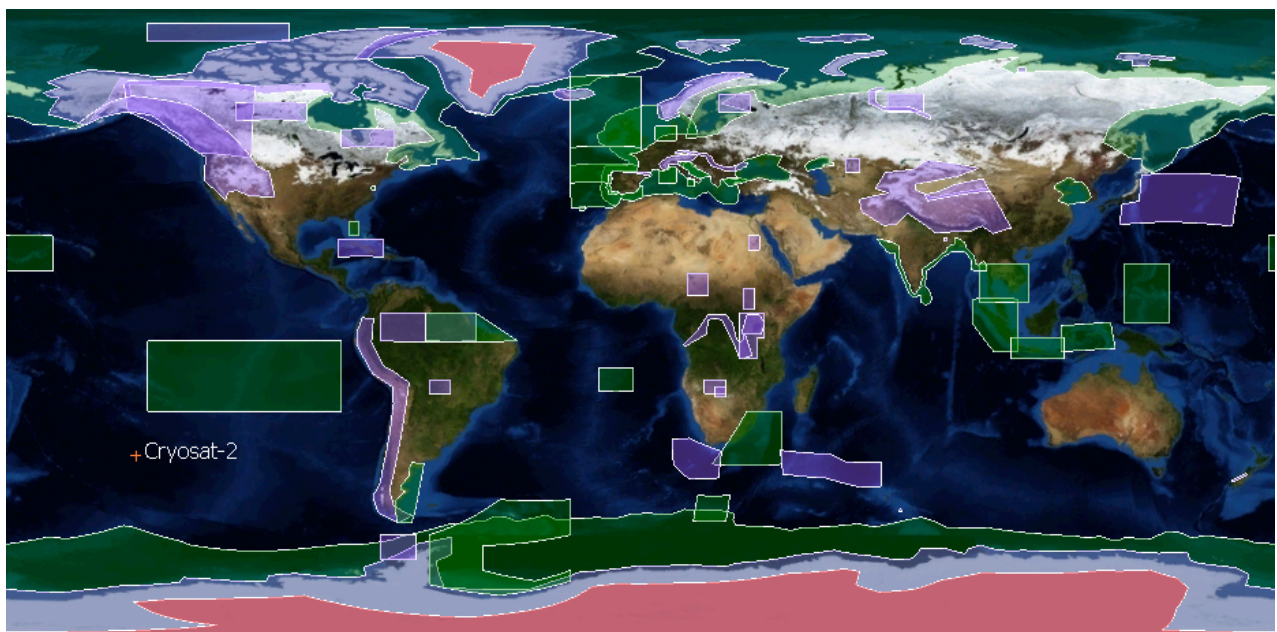


FIGURE 1: CRYOSAT-2 MODE MASK VERSION 3.4 SHOWING THE REGIONS WHERE THE ALTIMETER OPERATES IN SARIN (PURPLE), SAR (GREEN) AND LRM MODE (SOURCE: ESA)

Being mutually exclusive, only one mode is available at any given time. Hence, simultaneous measurements in Cryosat-2 LRM and Cryosat-2 SAR mode over the same surface are not possible. Instead, comparison between SAR and LRM relies on either, crossovers with other conventional altimeters, or on reconstructing LRM-type waveforms (“pseudo-LRM”) from the SAR data in a process known as SAR reduction or RDSAR (see Section 4 and Appendix E for a discussion of the RDSAR

² Further discussion of the Cryosat-2 operating modes is found in Section 4.



methods; see Section A.2 for examples of comparisons of LRM, P-LRM and SAR based on Cryosat-2 data).

While Cryosat-2 provides valuable altimetry data over the ocean, it is not an oceanographic mission. The first ocean altimetry mission featuring SAR mode will be the European GMES/Copernicus Sentinel-3 mission.

The SAR mode on Sentinel-3 will operate in “closed-burst” (see Section 4) similar to that used on Cryosat-2. As discussed in this document, while SAR mode on Sentinel-3 will deliver improved performance for ocean altimetry compared to conventional missions, its closed-burst SAR mode operation will not allow it to take full advantage of the benefits of SAR mode altimetry over ocean that can be achieved with the interleaved mode proposed for Jason-CS.



4. LRM AND SAR MODES: CLOSED BURST VS INTERLEAVED OPERATION AND TRANSFORMATION TO PSEUDO-LRM

This section provides a high-level summary of LRM, SAR “Closed-Burst” and SAR “Interleaved” modes of operation, and of the transformation of SAR mode data into LRM waveforms. A fuller discussion of these topics can be found in Appendix D and Appendix E respectively.

4.1. LRM AND SAR MODES: CLOSED BURST VS INTERLEAVED OPERATION

Figure 2 gives a schematic representation of the chronograms of the signals in each mode and lists the missions operating in each mode.

In LRM, pulses are transmitted and received continuously, using a low PRF to ensure that successive pulses are only partially correlated and that noise reduction can be achieved through incoherent averaging. The upper bound for the PRF is the so-called Walsh limit (Walsh, 1982) which is of the order of 1800 waveforms per second. In LRM, the transmitted and received pulses are interleaved, and this has been the case for all conventional altimeter missions (Figure 2, top).

In SAR mode as designed for CryoSat-2 and Sentinel-3, the pulses are transmitted and received in bursts of 64 pulses. The PRF within the burst is high, so that successive pulses within the bursts are correlated. For Cryosat-2, the PRF within each burst is approximately 18kHz, and each burst has a duration of about 3.5ms. The interval between bursts of received data is about 11.8ms, which implies that 70% of the opportunity to make measurements is not used. This form of the SAR mode is known as “closed burst” because, unlike interleaved, the reflections arrive back at the radar (as a received burst) after each transmitted burst has finished (Figure 2, middle).

The CryoSat-2 PRF was chosen to be about 18 kHz. However, it was shown (Raney, 2010) that such a high PRF is not required for an altimeter viewing the ocean from directly above. A PRF of the order of 9 kHz would suffice to achieve pulse-to-pulse coherence, and be low enough to allow space between transmitted pulses to allow interleaved transmitted and received pulse (Figure 2, bottom). This is what is proposed for Jason-CS and is known as “interleaved” mode (Phalippou *et al.*, 2012).

Interleaved SAR is predicted to deliver yet further range noise reduction even compared to closed-burst SAR (see Section A.6). There is however another result that is of more general significance: Interleaved SAR allows comparison between SAR and statistically equivalent LRM waveforms, which closed-burst SAR does not: it is impossible to generate “pseudo-LRM” (P-LRM) waveforms from closed-burst SAR-mode data that are statistically equivalent to waveforms obtained in LRM mode under the same viewing and sea-state conditions.

This has a direct bearing on Jason-CS, for which a major requirement is to guarantee continuity between measurements from Jason-CS and the 20-year heritage of measurements from earlier (LRM) missions on the same orbit. That requirement cannot be satisfied if Jason-CS uses the closed-burst SAR mode. Further, Jason-CS is required to support continuity across missions, so that its measurements may be quantitatively compared to LRM data from other altimeters at crossovers, for example. This requirement also cannot be met if Jason-CS uses only the closed burst architecture.



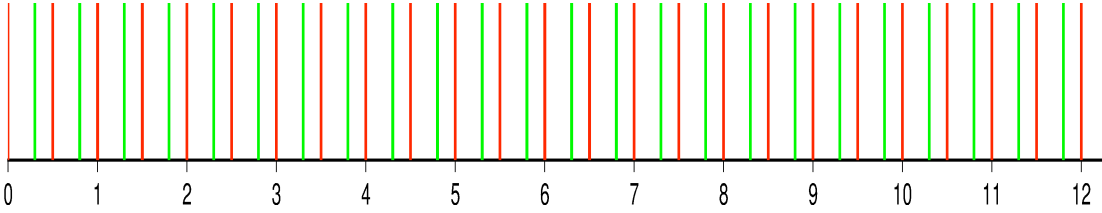
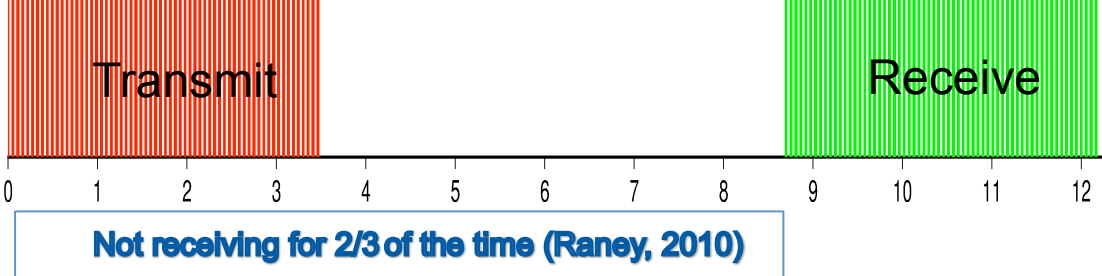
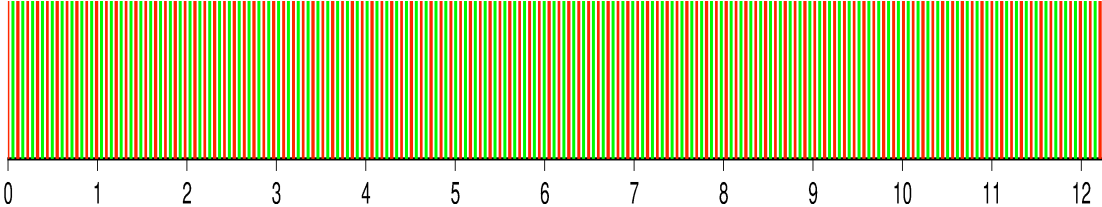
OPERATION MODE	CHRONOGRAM	ALTIMETRIC MISSIONS
Low Resolution Mode (LRM) Low PRF (1-4kHz) Continuous Tx/Rx		All past ocean altimeter missions Cryosat-2 LRM AltiKa Jason-3
SAR Closed-Bursts High PRF (~20 kHz) Tx/Rx in bursts		Cryosat-2 SAR Sentinel-3
SAR "Interleaved" Moderate PRF (~ 9 kHz) Continuous Tx/Rx		Jason-CS

FIGURE 2: CHRONOGRAMS FOR LRM (TOP), SAR CLOSED BURST MODE (MIDDLE) AND SAR INTERLEAVED MODE (BOTTOM) (SOURCE: ADAPTED FROM SMITH ET AL., 2013)



4.2. PSEUDO-LRM IN SAR CLOSED-BURST

Transformation from LRM to SAR-mode data is not possible. Inversely, transformation from SAR mode data to (pseudo-) LRM data is possible, but as noted above, only approximately in the case of closed-burst SAR. The transformation process is known as SAR reduction, or RDSAR (Martin-Puig *et al.*, 2008; Martin-Puig *et al.*, 2010; Boy *et al.*, 2011; Scharroo *et al.*, 2012; Labroue *et al.*, 2013), which produces pseudo-LRM waveforms that are intended to embody the same Brown-like appearance as true LRM waveforms, and therefore can be retracked with existing LRM retrackers.

The RDSAR alternatives are described in Appendix E, while examples of comparisons of LRM, P-LRM and SAR based on Cryosat-2 data are presented in Section A.2.



5. ADVANCES WITH SAR ALTIMETRY OVER THE OCEAN

This section guides the reader through the technical material provided in the subsequent appendices that demonstrate recent advances in ocean altimetry achieved with SAR mode on Cryosat-2.

Section A.1 presents evidence of the reduced measurement noise in SAR mode compared to P-LRM and LRM from Jason-2. Various independent groups working with different datasets and SAR retracking methods consistently report 1Hz range noise around 1 cm for significant wave height of 2 metres (compared to 1.6 cm for LRM). Section A.1.3 presents the improvements in range noise with interleaved SAR on Jason-CS, which is expected to further reduce to 0.5 cm for 2m significant wave height.

Section A.2 reports the results of global comparisons of LRM, P-LRM and SAR mode based on Cryosat-2 data performed by several groups using different retrackers and RDSAR methodologies. It is shown that useful ocean parameters can be extracted by retracking Cryosat-2 P-LRM waveforms, albeit with the expected increase in noise. Transitions between LRM and P-LRM are smooth, but the lack of a SSB model in SAR mode currently makes it impossible at present to assess LRM/SAR transitions in sea surface height anomalies.

Section A.3 shows the important results by Boy *et al.* (2012) who compare sea level anomaly (SLA) spectra in LRM, P-LRM and SAR mode. While LRM and P-LRM display a spectral “hump” for ocean length scales between 7 and 100 km, the SLA spectrum for Cryosat-2 SAR does not, suggesting that SAR altimetry provide physically meaningful information on SLA down to much shorter lengths scales than is possible with LRM or P-LRM.

Section A.4 gives examples of the improved altimeter data quality and increased data availability in SAR mode in the vicinity of land, with SAR altimetry delivering high quality data up to within 1 km of the coast and over inland bodies of waters.

Section A.5 presents the results of validation of SAR SWH against buoys around the UK and in the German Bight, indicating that SAR can provide SWH data at least as good as LRM over a wide range of sea states. The retrieval of good SAR SWH is however dependent on appropriate processing of the L1B multi-looked waveforms and accurate information about platform mispointing to use as input to the SAR retracker.

Finally, appendix B reviews the considerable efforts over the past three years by various groups in developing models and methods to retrack SAR waveforms, demonstrating that there is now a high level on confidence in the ability to extract geophysical information from SAR altimeter waveforms.



6. CONCLUSIONS

This review provides an overview of the state of knowledge for SAR altimetry over the ocean based on research reported over the last few years (2010-2013). It is clear that SAR altimetry has attracted considerable attention and that remarkable progress has been made in a short space of time on many aspects of the subject.

There is increasing consensus between various independent investigation teams that SAR altimetry over the ocean leads to significant performance improvements when compared to even the best available conventional radar altimetry. The results are evident in reduced measurement uncertainty (Section A.1), improved performance in coastal regions (Section A.3), and the ability to retrieve useful ocean parameters from pseudo-LRM data³ (Section A.2).

The convergence of results from different groups using different SAR waveform retracers (Appendix B) indicates that there is now a high level of confidence in the ability to retrieve geophysical data from SAR mode altimetry over ocean. There is also compelling evidence about the improved spectral information content for Sea Level Anomaly at the ocean mesoscale with SAR altimetry (Section A.4).

Several issues remain open, specifically the sensitivity to mispointing, the need for a sea state bias model in SAR mode, and the effects of swell and swell direction on SAR waveforms when observed through the fine along-track footprint native to the SAR mode (Appendix C). However, if the Jason-CS SAR mode is interleaved, then such issues disappear since the resulting SAR mode data can be transformed seamlessly into LRM data.

CryoSat-2 pseudo-LRM data are not equivalent to real LRM data (Appendix E). Sentinel-3 will in future provide more SAR data over larger regions, perhaps even globally, but its SAR operation in closed-burst mode will yield pseudo-LRM with the same increased measurement uncertainty as is seen for Cryosat-2. The fundamental fact remains: closed burst SAR mode data cannot be transformed to generate pseudo-LRM waveforms that are statistically equivalent to real LRM waveforms.

Lack of equivalent P-LRM waveforms from closed burst SAR mode data precludes direct SAR/LRM cross-calibration. This fact jeopardizes the self-calibration potential of a closed burst SAR mode altimeter, and compromises attempts to relate - with sufficient confidence and precision - the closed-burst SAR sea level measurements to the existing sea level record. Adopting closed-burst SAR on Jason-CS would compromise the continuity of the high-precision sea level 20-year time series.

SAR interleaved would realize the theoretically optimal performance expected from a SAR mode altimeter, while ensuring continuity with conventional altimeters. As this report explains, the SAR interleaved mode is essential since it is the only method that would assure continuity between the SAR mode aboard Jason-CS, and contemporaneous and prior conventional altimetric missions.

Following this review, it is recommended that:

³ Subject to the inherent limitations imposed by the closed burst SAR mode used by CryoSat-2



- Jason-CS should be implemented with the SAR Mode, which is the state-of-the art in radar altimetry, having been demonstrated in orbit with CryoSat-2, with significant benefits for many ocean applications.
- The Jason-CS SAR mode should be interleaved, since it is the only mode of operation that delivers SAR mode data that can be successfully transformed into pseudo-LRM data that are statistically equivalent to true LRM data.
- The Jason-CS SAR mode should be interleaved to assure that SAR mode data could be transformed into conventional LRM data, thus providing a foundation for self-calibration of the SAR altimeter against LRM.
- The Jason-CS SAR mode should be interleaved so that LRM products could be generated that would support statistically significant comparisons with LRM products from other missions.
- The Jason-CS SAR mode should be interleaved so that its products could provide seamless continuity with the sea level measurement record established by prior altimeters in the TOPEX orbit, and
- The Jason-CS altimeter should implement a SAR interleaved mode of operation so that its measurements satisfy its prime mission requirements for long-term continuity of sea level monitoring.

APPENDIX A. IMPROVED PERFORMANCE OF SAR MODE ALTIMETRY OVER OCEAN

The availability of SAR mode waveforms from Cryosat-2 has led to growing observational evidence of the improved performance of SAR altimetry compared to conventional altimetry. Given the relative novelty of SAR altimetry, the evidence is by no means complete and there are still open issues that remain the object of active research. These are presented in Appendix C.

A.1. REDUCED MEASUREMENT NOISE IN SAR MODE

A.1.1. CRYOSAT-2 SAR WITH CRYOSAT-2 P-LRM

Several studies have quantified the noise reduction on range and SWH with SAR using Cryosat-2 data. Based on pseudo-LRM and SAR waveforms reconstructed from the same Cryosat-2 FBR Level 0 products, Phalippou & Demeestere (2011) provide the most direct comparison of the capabilities of SAR mode and LRM. Analyses were performed over a wide range of SWH conditions, leading to plots of noise on range and SWH as a function of SWH (Figure 3; SWH plot not shown). The SAR range and SWH were retrieved using the numerical SAR waveform retracker (see Section B.1) by Phalippou & Enjolras (2007).

These results confirmed the two-fold noise reduction in SAR mode compared to LRM that had been predicted by earlier simulations (Jensen & Raney, 1998), with range and SWH noise at 1Hz equal to 0.8 cm and 4 cm respectively at a significant wave height of 2 metres.

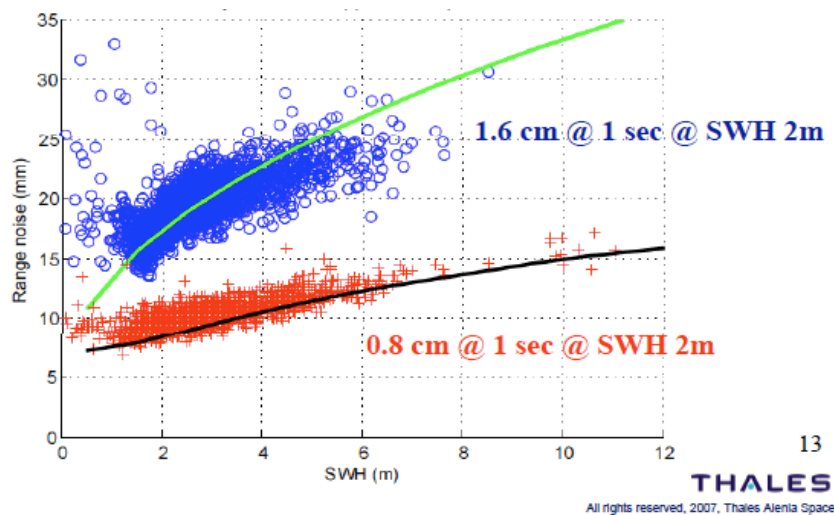


FIGURE 3: NOISE AT 1HZ FOR RETRIEVED RANGE AS A FUNCTION OF SIGNIFICANT WAVE HEIGHT FOR “LRM-LIKE” (I.E. SCALED P-LRM; BLUE) AND SAR MODE (RED). THE P-LRM AND SAR WAVEFORMS WERE DERIVED FROM THE SAME CRYOSAT-2 FULL-BIT-RATE PRODUCTS, AND SAR WAVEFORMS WERE RETRACKED WITH THE NUMERICAL MODEL BY PHALIPPOU & ENJOLRAS (2007) (SOURCE: PHALIPPOU & DEMEESTERE, 2011).

Using a similar approach, Giles *et al.* (2012) presented similar findings, albeit based on the semi-analytical SAR retracking model (see Section B.2) by Wingham *et al.* (2004), and reporting slightly larger 1Hz noise for both range (1.1 cm) and SWH (7.5cm) at a significant wave height of 2 metres (Figure 4).

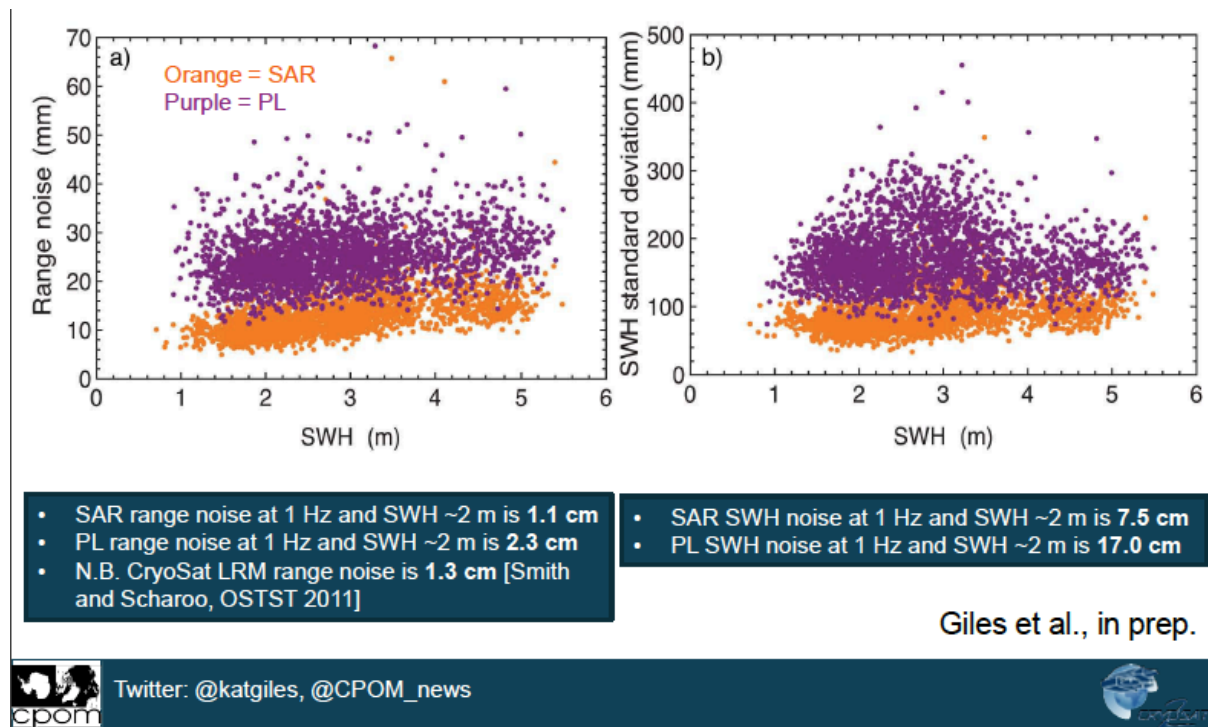


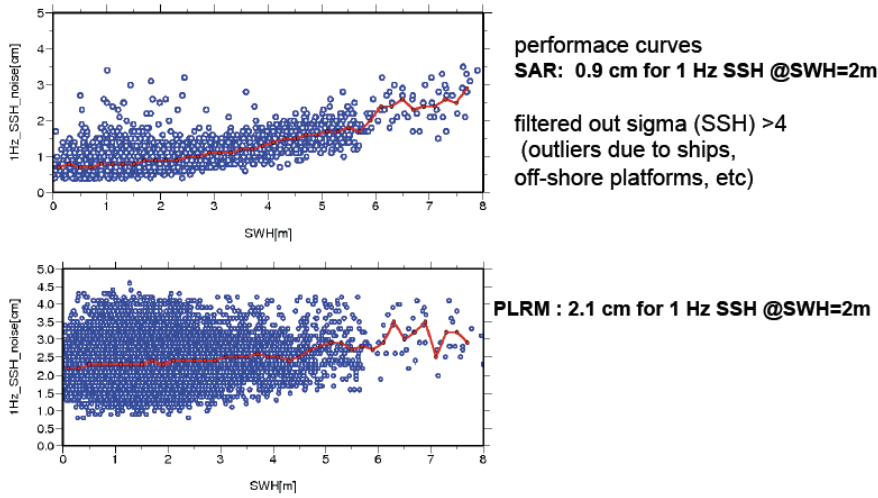
FIGURE 4: NOISE AT 1HZ FOR RETRIEVED RANGE (LEFT) AND SIGNIFICANT WAVE HEIGHT (RIGHT) AS A FUNCTION OF SIGNIFICANT WAVE HEIGHT FOR PSEUDO-LRM (PURPLE) AND SAR (ORANGE). THE P-LRM AND SAR WAVEFORMS WERE DERIVED FROM THE SAME CRYOSAT-2 FULL-BIT-RATE PRODUCTS AND SAR MODE WAVEFORMS WERE RETRACKED WITH THE SEMI-ANALYTICAL MODEL BY WINGHAM *ET AL.*, 2004 (SOURCE: GILES *ET AL.*, 2012)

Finally, Dinardo & Fenoglio-Marc (2013) recently confirmed these findings for Cryosat-2 SAR data obtained in the German Bight. In this case, the FBR-derived multi-looked SAR waveforms were retracked with the fully analytical SAMOSA3 retracker (Section B.3). In these analyses, the Cryosat-2 SAR 1Hz noise was respectively equal to 0.9 cm for SSH and 6.5 cm for SWH at a significant wave height of 2 metres.



Introduction Methods | **Results** | Conclusions

Precision SSH : SAR and RADS/PLRM

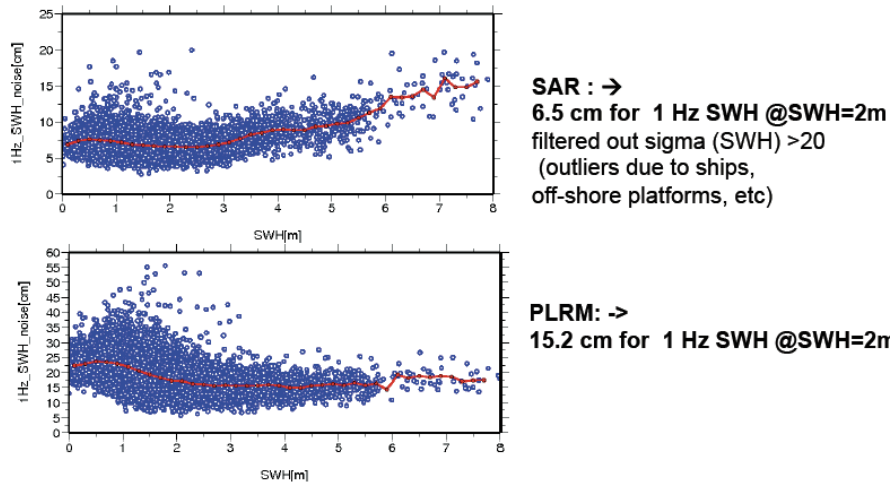


PSGD Altimetrics serco eesa deimos TECHNISCHE UNIVERSITÄT DARMSTADT Southampton 26-27 June 2013 9

FIGURE 5: NOISE AT 1HZ FOR CRYOSAT-2 RETRIEVED SSH IN SAR MODE (TOP) AND FROM PSEUDO-LRM WAVEFORMS (BOTTOM) AS A FUNCTION OF SIGNIFICANT WAVE HEIGHT IN THE GERMAN BIGHT AREA. (SOURCE: DINARDO & FENOGLIO-MARC, 2013)

Introduction Methods | **Results** | Conclusions

Precision SWH : SAR & PLRM



PSGD Altimetrics serco eesa deimos TECHNISCHE UNIVERSITÄT DARMSTADT Southampton 26-27 June 2013 10

FIGURE 6: NOISE AT 1HZ FOR CRYOSAT-2 RETRIEVED SSH IN SAR MODE (TOP) AND FROM PSEUDO-LRM WAVEFORMS (BOTTOM) AS A FUNCTION OF SIGNIFICANT WAVE HEIGHT IN THE GERMAN BIGHT AREA. (SOURCE: DINARDO & FENOGLIO-MARC, 2013)



A.1.2. CRYOSAT-2 SAR VERSUS JASON-2 LRM

Using a totally different approach, Gommenginger *et al.* (2011) confirmed the reduced noise of SAR over LRM by comparing Cryosat-2 SAR data against Jason-2 over specific regions and periods. As direct comparison between the two satellites is seldom possible (the orbits of Cryosat-2 and Jason-2 offer very few opportunities for exact collocations of the satellites in time), the noise on sea surface height and SWH for Cryosat-2 SAR and Jason-2 LRM is plotted against SWH for comparison. Figure 7 shows the Cryosat-2 SAR mode 20Hz retrieved SSH and SWH obtained over the Norwegian Sea between July 2010 and July 2011.

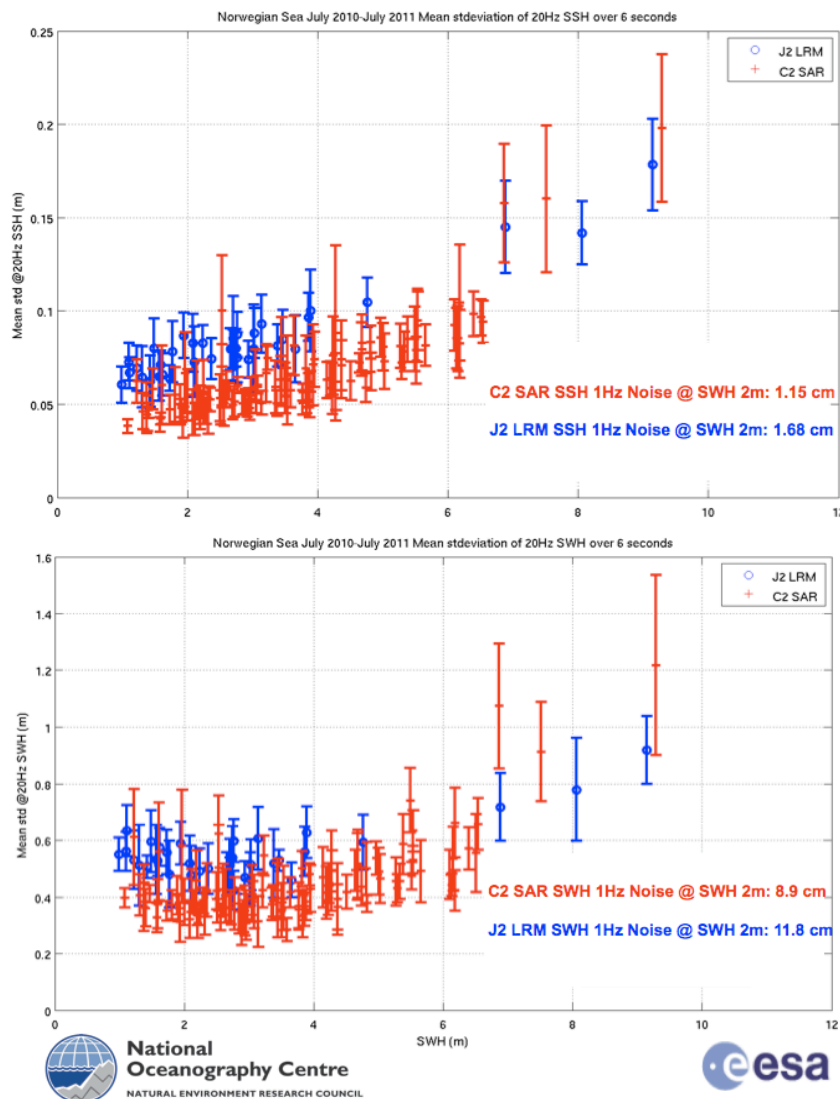


FIGURE 7: NOISE AT 20HZ (STD) FOR RETRIEVED SEA SURFACE HEIGHT (TOP) AND SIGNIFICANT WAVE HEIGHT (BOTTOM) AS A FUNCTION OF SIGNIFICANT WAVE HEIGHT FOR JASON-2 L2 LRM (BLUE) AND CRYOSAT-2 SAR (RED). THE SAR DATA CORRESPONDS TO ESA OPERATIONAL PRODUCTS FOR BASELINE A, RETRACKED WITH THE FULLY ANALYTICAL SAMOSA3 MODEL (SOURCE: GOMMENGINGER ET AL., 2011)



The data were retracked with the SAMOSA3 SAR retracker, with platform mispointing as input to the retracker. The error bars represent the variability of the noise over 6 seconds of data.

The 1Hz noise for Cryosat-2 SAR for sea surface height and SWH is equal to 1.15 cm and 8.9 cm respectively at a significant wave height of 2 metres, compared to 1.68 cm and 11.8 cm for Jason-2. The noise improvement for Cryosat-2 SAR against Jason-2 LRM is therefore only by a factor of 1.5, instead of by a factor of 2 as seen above. This small under-performance is largely attributed to processing choices in the ESA operational Cryosat-2 SAR L1B processing chain being optimised for sea ice echoes, leading to smearing of the leading edge of SAR waveforms over ocean.

A.1.3. SUB-CM RANGE NOISE WITH SAR INTERLEAVED MODE ON JASON-CS

The predicted noise performance of SAR interleaved mode for range and SWH retrieval have been estimated for Jason-CS by Phalippou *et al.* (2012). Based on the methodology validated previously against Cryosat-2 SAR data (Figure 3), the 1Hz range noise for Jason-CS in SAR interleaved is estimated around 0.5 cm (Figure 8) for a SWH of 2 m. Thus, SAR interleaved mode should deliver yet further improvement in sea surface height retrieval, beyond the 0-8-1 cm range noise already observed with Cryosat-2 closed-burst SAR, and well beyond the 1.6 cm 1Hz range noise of conventional altimeters (Figure 7).

■ Range noise estimation

- Methodology and echo modeling validated against in flight SAR-SIRAL data
- Numerical model of echoes including azimuth aliasing + speckle / thermal noise
- RMC effect has also been assessed

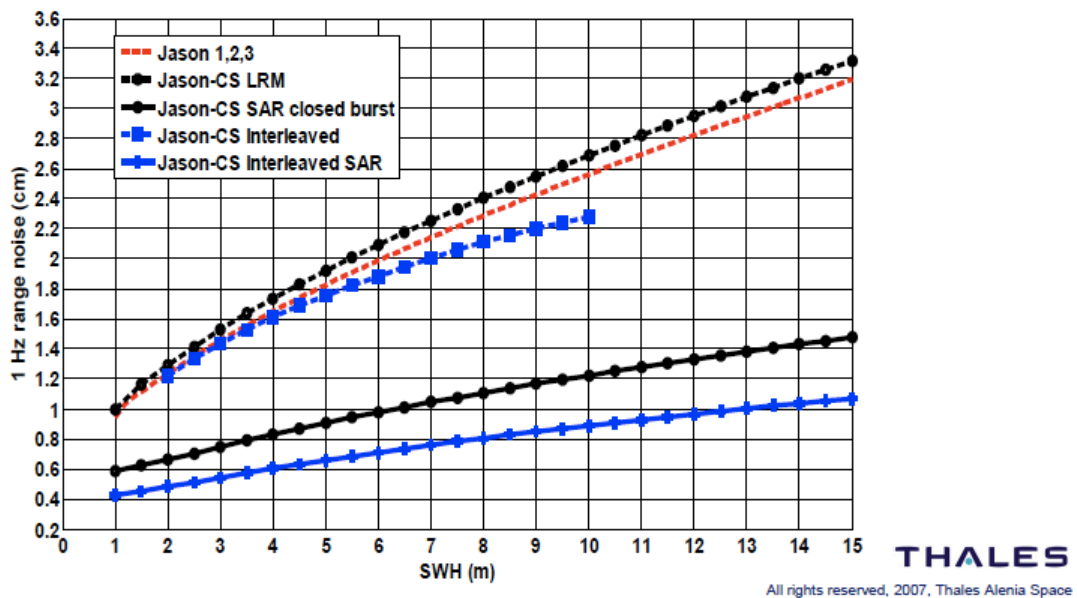


FIGURE 8: PREDICTED 1HZ RANGE NOISE AS A FUNCTION OF SIGNIFICANT WAVE HEIGHT FOR SAR “CLOSED-BURST” (LOWER BLACK CURVE) AND SAR “INTERLEAVED” (LOWER BLUE CURVE) MODE OF OPERATIONS ON JASON-CS (SOURCE: PHALIPPOU *ET AL.*, 2012)

A.2. GLOBAL COMPARISONS OF CRYOSAT-2 LRM, P-LRM AND SAR DATA

The SAR reduction methodology has now been applied to Cryosat-2 SAR waveforms globally as reported by Scharroo *et al.* (2012) and Boy *et al.* (2012). These analyses permit an assessment of the continuity of retrieved ocean properties at LRM/SAR transitions.

After much effort dealing with unresolved processing errors in the ESA Cryosat-2 products (e.g. erroneous AGC corrections), Scharroo *et al.* (2013) were able to demonstrate continuity of ocean properties across LRM/SAR transitions, without jumps or offsets (Figure 9). The results also highlight the expected increased noise of the P-LRM retrieved parameters, in particular SSH and SWH (Figure 9, 2nd and 3rd panels from the right), for SAR altimeters operating in sub-optimal closed-burst mode (such as Cryosat-2 and Sentinel-3).

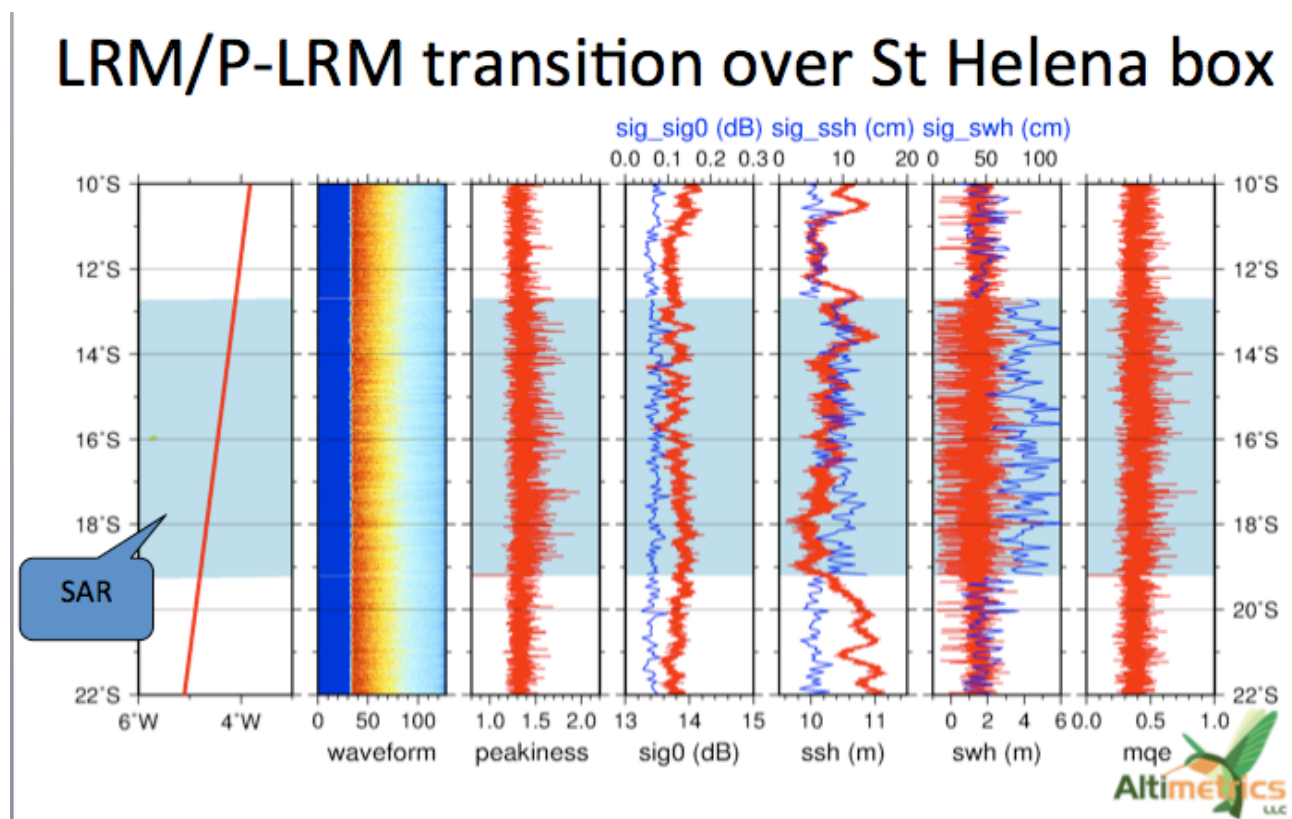


FIGURE 9: CRYOSAT-2 LRM AND P-LRM RETRACKED OCEAN PARAMETERS ACROSS THE SAR BOX OVER ST HELENA ISLAND (SOUTH ATLANTIC), SHOWING (FROM LEFT TO RIGHT) THE LATITUDE/LONGITUDE OF THE SAR BOX, THE LRM AND P-LRM WAVEFORMS, WAVEFORM PEAKINESS, AND THE MEAN (RED) AND STANDARD DEVIATION (BLUE) OF: BACKSCATTER COEFFICIENT (SIGMA0), SEA SURFACE HEIGHT, AND SIGNIFICANT WAVE HEIGHT. THE LAST PANEL ON THE RIGHT SHOWS A MEASURE OF THE FIT BETWEEN THE WAVEFORMS AND THE MODEL. BOTH LRM AND P-LRM WAVEFORMS WERE RETRACKED WITH THE MLE3 BROWN MODEL IMPLEMENTED AT NOAA (SOURCE: SCHARROO *ET AL.*, 2013)

The availability of global Cryosat-2 data in LRM and P-LRM enabled the development of dedicated Sea State Bias models for both modes. In turn, this makes it possible to produce maps of sea level

anomaly (Figure 10). Apart from the missing data over zones where Cryosat-2 operates in SARIn over the ocean, there are no signs of discontinuity in SLA or SWH (not shown) at LRM/SAR transitions of the Cryosat-2 mode mask (e.g. central Pacific or Agulhas region).

LRM+PLRM – Sea Level Anomaly

sla (lrm1r) – subcycle 029 – 2012/06/11 – 2012/07/08

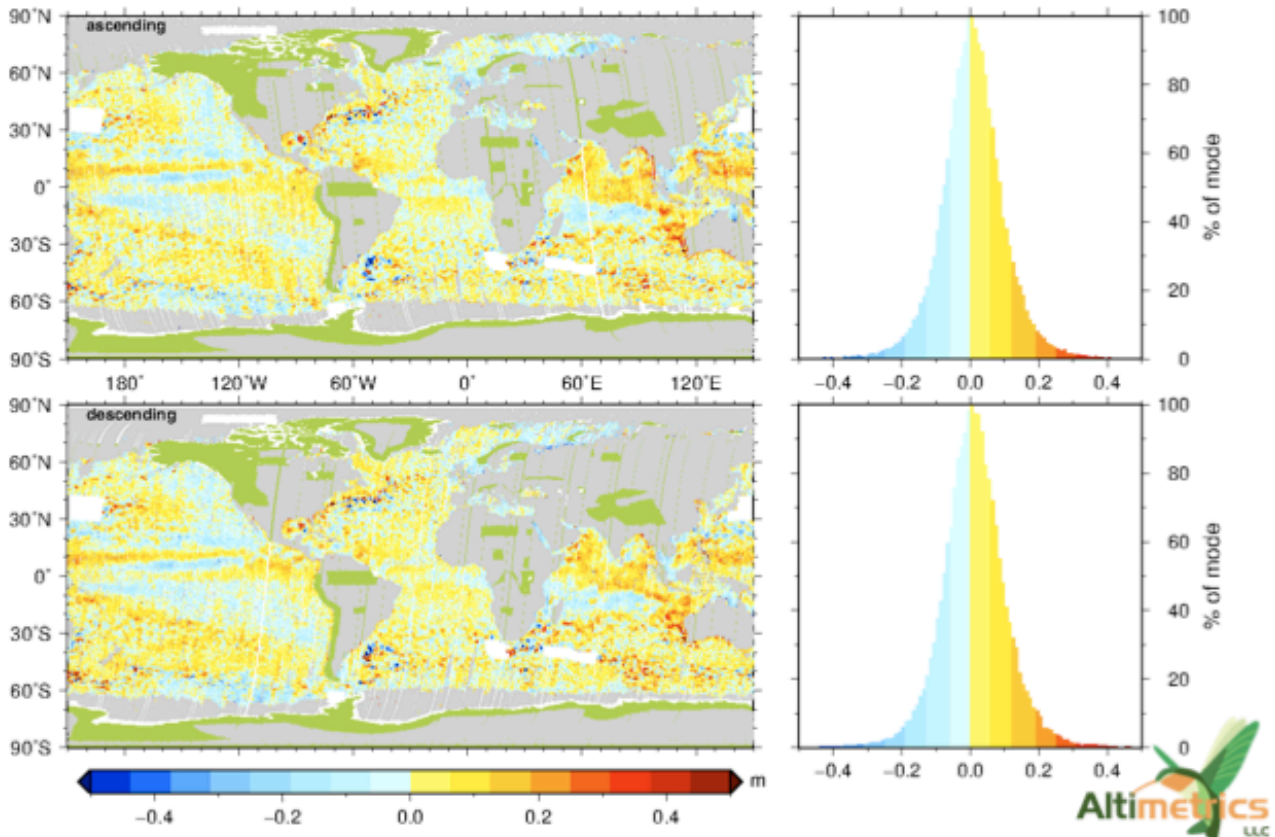


FIGURE 10: GLOBAL MAPS OF SEA LEVEL ANOMALY FOR COMBINED CRYOSAT-2 LRM AND P-LRM DATA. THE CRYOSAT-2 DATA WERE RETRACKED WITH THE ML3 MODEL IMPLEMENTED AT NOAA. THE SLA ARE CORRECTED FOR GEOPHYSICAL EFFECTS, INCLUDING CORRECTIONS FOR SEA STATE BIAS BASED ON MODELS DEVELOPED SPECIALLY FOR CRYOSAT-2 LRM AND P-LRM (SOURCE: SCHARROO *ET AL.*, 2013)

Figure 11 shows a zoomed-in view over the Atlantic of similar global SLA analyses presented by Boy *et al.* (2012) based on LRM, P-LRM and SAR data from the CNES Cryosat-2 Prototype products (CPP). Here again, there is no evidence of discontinuity in SLA between the LRM and P-LRM (Figure 11, bottom right).

In addition, Figure 11 top right shows the SLA for LRM and SAR. Again, no marked discontinuity can be seen between LRM and SAR SLA at the LRM/SAR transitions. However, a closer look at SLA profiles



across a LRM/SAR transition in the Agulhas region (Figure 12) shows that there is a small but discernible jump. As noted by Boy *et al.*, 2012, the exact bias between LRM and SAR is difficult to quantify at this stage, since there is no model to correct the SAR SLA for SSB.

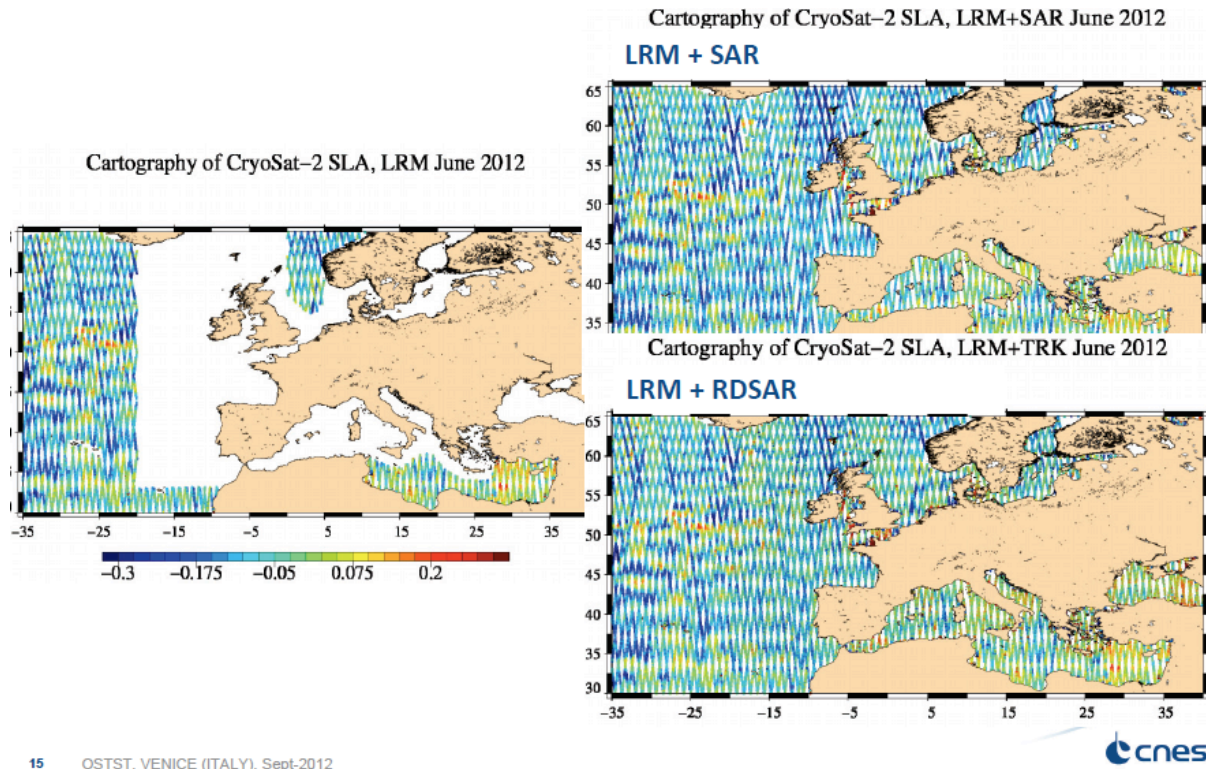
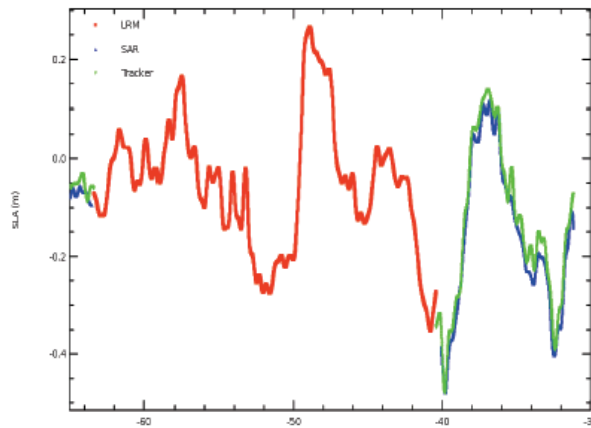


FIGURE 11: ZOOMED-IN VIEW OF SEA LEVEL ANOMALY OVER THE NORTH-WEST ATLANTIC FOR (LEFT) CRYOSAT-2 LRM (TOP RIGHT) COMBINED CRYOSAT-2 LRM AND SAR AND (BOTTOM RIGHT) COMBINED CRYOSAT-2 LRM AND P-LRM. ALL DATA ARE FROM THE CNES CPP PRODUCTS. THE CRYOSAT-2 SAR DATA WERE RETRACKED WITH THE NUMERICAL SAR WAVEFORM MODEL BY BOY *ET AL.*, 2012. (SOURCE: BOY *ET AL.*, 2012)



Track 130 over Agulhas current

Red: LRM
Blue: SAR
Green: RDSAR



- Good transition between LRM (red) and SAR (blue) measurements.
- Analysis still on going to analyse precisely bias between LRM and SAR SLA. **Hard to do since SSB is applied on LRM results but none on SAR.**

21 OSTST, VENICE (ITALY), Sept-2012



FIGURE 12: CRYOSAT-2 SEA LEVEL ANOMALY PROFILES AT A LRM/SAR TRANSITION IN THE AGULHAS REGION SHOWING SLA FOR LRM (RED), P-LRM (GREEN) AND SAR (BLUE). THE FIGURE SHOWS THE GOOD CORRESPONDENCE BETWEEN SAR AND P-LRM AND THE SLIGHT JUMP IN SLA BETWEEN LRM AND SAR DUE (IN PART) TO THE LACK OF SSB CORRECTION FOR SAR SLA (SOURCE: BOY ET AL., 2012)



A.3. IMPROVED SEA SURFACE HEIGHT SPECTRA AT SHORT OCEAN WAVELENGTHS

Boy *et al.* (2012) reported the first example of sea level anomaly (SLA) spectrum obtained for Jason-2 LRM, Cryosat-2 SAR and Cryosat-2 P-LRM (Figure 13).

These analyses revealed several important results:

- the spectra in the three modes are superposed for ocean length scales greater than 100km, meaning that SAR and P-LRM mode contain the same information at medium to large length scales without detrimental errors
- a white noise plateau is visible for all spectra for length scales between 600 meters and 3 km approximately. The noise floor for Cryosat-2 P-LRM is higher than for Jason-2 LRM by a factor of $\sqrt{3}$ (as expected) while the noise floor for Cryosat-2 SAR is lower than for Jason-2 LRM by about 30%.
- Finally, and most importantly, for length scales between 7 and 100 km (ocean mesoscale), the spectra for Jason-2 LRM and Cryosat-2 P-LRM both feature a “hump”, while the Cryosat-2 SAR spectrum does not. This suggests that SAR altimetry provides SLA which spectral information content is physically more meaningful.

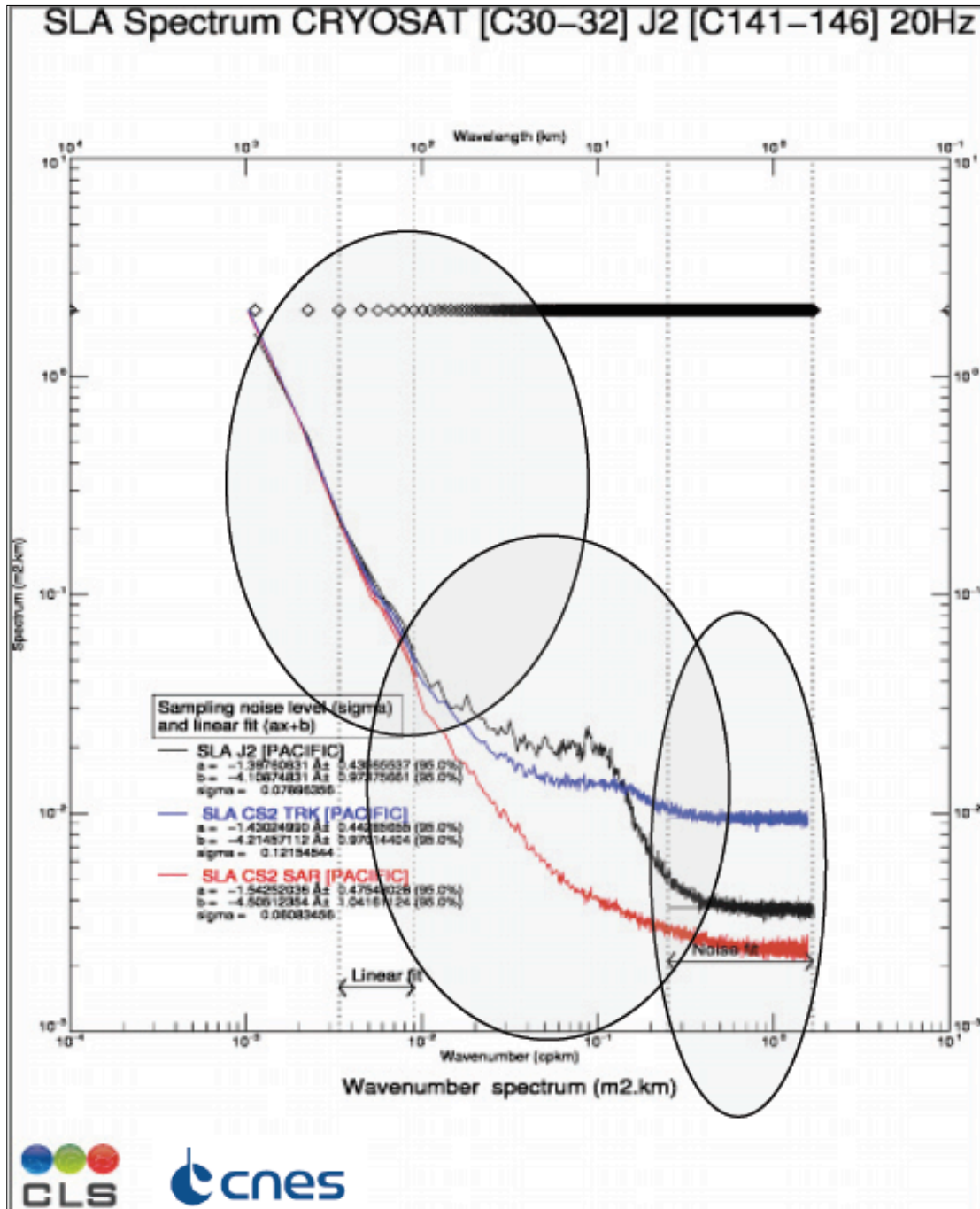


FIGURE 13: SEA LEVEL ANOMALY SPECTRUM FOR JASON-2 LRM (BLACK), CRYOSAT-2 SAR (RED) AND CRYOSAT-2 P-LRM OVER THE PACIFIC OCEAN. SAR WAVEFORMS WERE RETRACKED WITH THE NUMERICAL MODEL BY BOY ET AL., 2012 (SOURCE: BOY ET AL., 2012)



A.4. IMPROVED ALTIMETER DATA QUALITY AND AVAILABILITY IN COASTAL REGIONS

The finer along-track spatial resolution of SAR altimetry (~ 300 meters instead of few km for LRM) is also expected to yield better performance in coastal regions due to reduced contamination of ocean waveforms by echoes from land. This excellent performance near land has been demonstrated with Cryosat-2 SAR data in many different regions, for example along the south coast of UK (Figure 14), where Cryosat-2 SAR gives valid measurements of SSH and SWH up to within 1 km of the coast.

Note that, as the spatial resolution of SAR mode across-track is the same as for LRM (i.e. a few km), SAR altimeter waveforms will be contamination by land in the same way as LRM when tracks run parallel to the coast (Dinardo *et al.*, 2011).



FIGURE 14: CRYOSAT-2 SAR SEA SURFACE HEIGHT PROFILES NEAR WEYMOUTH ON THE SOUTH COAST OF THE UK, SHOWING EXCELLENT ALTIMETRIC PERFORMANCE (WITHOUT JUMPS OR LOSS OF DATA) RIGHT UP TO THE COAST, AND INCLUDING OVER THE BODY OF INLAND WATER AROUND BROWNSEA ISLAND (SOURCE: GOMMENGINGER *ET AL.*, 2012B)

Figure 15 shows another example of an atoll in French Polynesia in the Western Pacific, which features overpasses by Cryosat-2 SAR (red) and Jason-2 LRM (blue) three days apart. The figure shows the poor quality and significant data loss for Jason-2 LRM (both SSH and SWH) as the satellite passes over the atoll, compared to the smooth and continuous measurements from Cryosat-2 SAR mode, which provides good data even over the atoll ring and the interior lagoon.



The bottom plot in Figure 15 shows SSH measured by the two satellites three days apart, illustrating once again the difficulty in comparing SAR and LRM from two different satellites. Here, the differences in SSH may be due to many factors, including differences in the quality of the orbits and geophysical corrections (e.g. no wet tropospheric correction on Cryosat-2), differences in environmental conditions on the days of the two satellite passes, and the lack of a Sea State Bias correction for Cryosat-2 SAR.

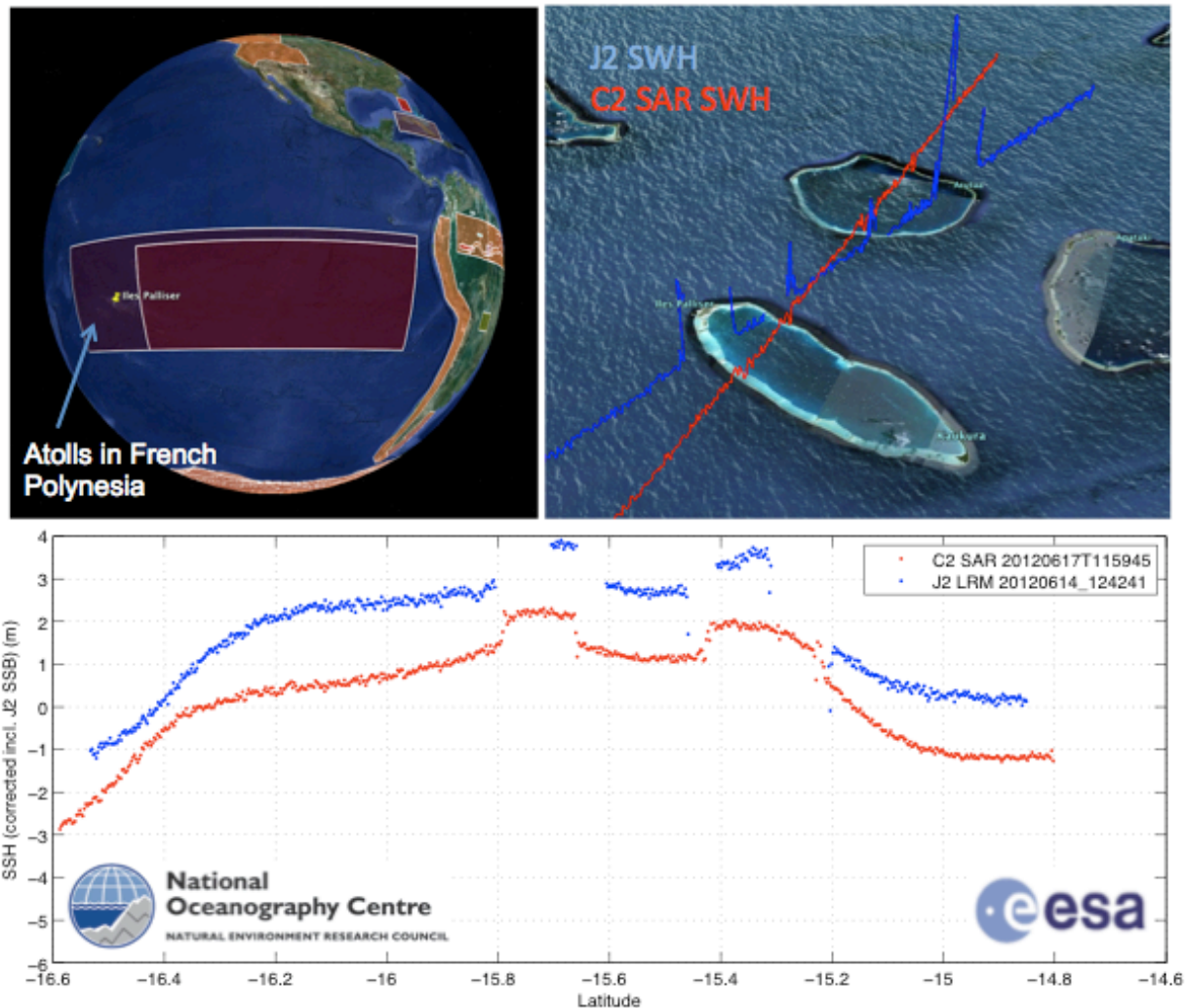


FIGURE 15: SEA SURFACE HEIGHT PROFILES FOR JASON-2 (BLUE) AND CRYOSAT-2 SAR (RED) OVER AN ATOLL OF THE PALLISER ISLANDS IN FRENCH POLYNESIA. THE TWO PASSES ARE THREE DAYS APART. TOP RIGHT SHOWS RETRIEVED SWH FOR BOTH SATELLITES, HIGHLIGHTING THE SUPERIOR DATA QUALITY AND AVAILABILITY FOR CRYOSAT-2 SAR NEAR LAND. BOTTOM PLOT SHOWS SEA SURFACE HEIGHT CORRECTED TO LEVEL 2. THE SAR SSH IS COMPUTED WITH L1B ORBIT AND NO CORRECTION FOR SEA STATE BIAS (SOURCE: COTTON *ET AL.*, 2013).

A.5. VALIDATION OF SAR SWH AGAINST BUOYS



Significant wave height retrieved from Cryosat-2 SAR waveforms has been validated against measurements from moored wave buoys provided by the UK Met Office on the European Continental shelf break (Figure 16). SWH was obtained by retracking ESA Cryosat-2 L1B SAR waveforms with the SAMOSA3 model, using the satellite platform mispointing as input to the SAR retracker. The Cryosat-2 data was selected within 50km of each buoy and collocated with buoy measurements within 30 minutes of the satellite overpass.

Analyses of the residuals based on ESA Cryosat-2 Baseline A products (July 2010-Dec 2011) produced reasonably small standard deviation (0.5m at 20Hz) and a small bias (0.295m) against buoys. There were also indications that SAR mode was not able to retrieve SWH below 0.8 meters.

The analyses were repeated with ESA Cryosat-2 Baseline B products (February 2012-onwards) after the ESA IPF processor changed to finer gate resolution in the waveforms with consequent truncation of the waveform trailing edge. For ESA Baseline B products, the residual standard deviation on 20Hz SWH against buoys reduced to 0.238m, while the bias increased to an unacceptable 0.896m.

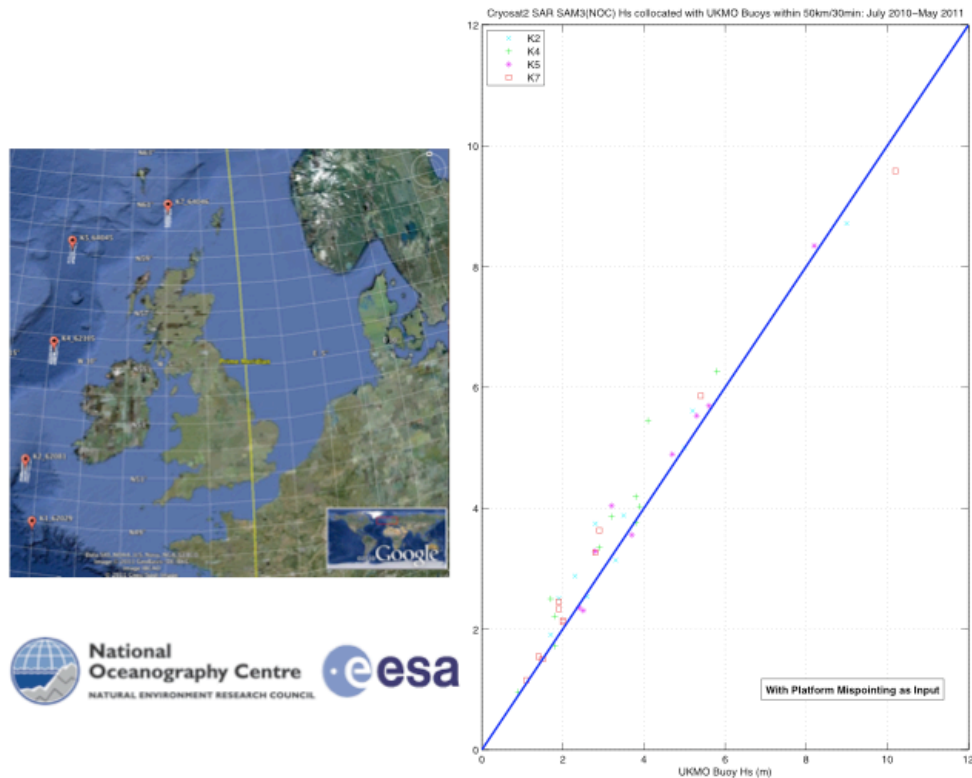


FIGURE 16: COMPARISON OF CRYOSAT-2 20HZ SAR RETRIEVED SIGNIFICANT WAVE HEIGHT AGAINST SWH MEASURED BY MOORED WAVE BUOYS FROM THE UK MET OFFICE ON THE EUROPEAN CONTINENTAL SHELF BREAK. THE SAR SWH WAS RETRIEVED WITH THE SAMOSA3 SAR OCEAN RETRACKER USING PLATFORM ACROSS-TRACK MISPOINTING ANGLE AS INPUT TO THE RETRACKER (CORRECTED FOR BIAS IN ROLL ANGLE AS ESTIMATED BY SCHARROO, 2011, PERS. COMM) (SOURCE: GOMMENGINGER ET AL., 2012)

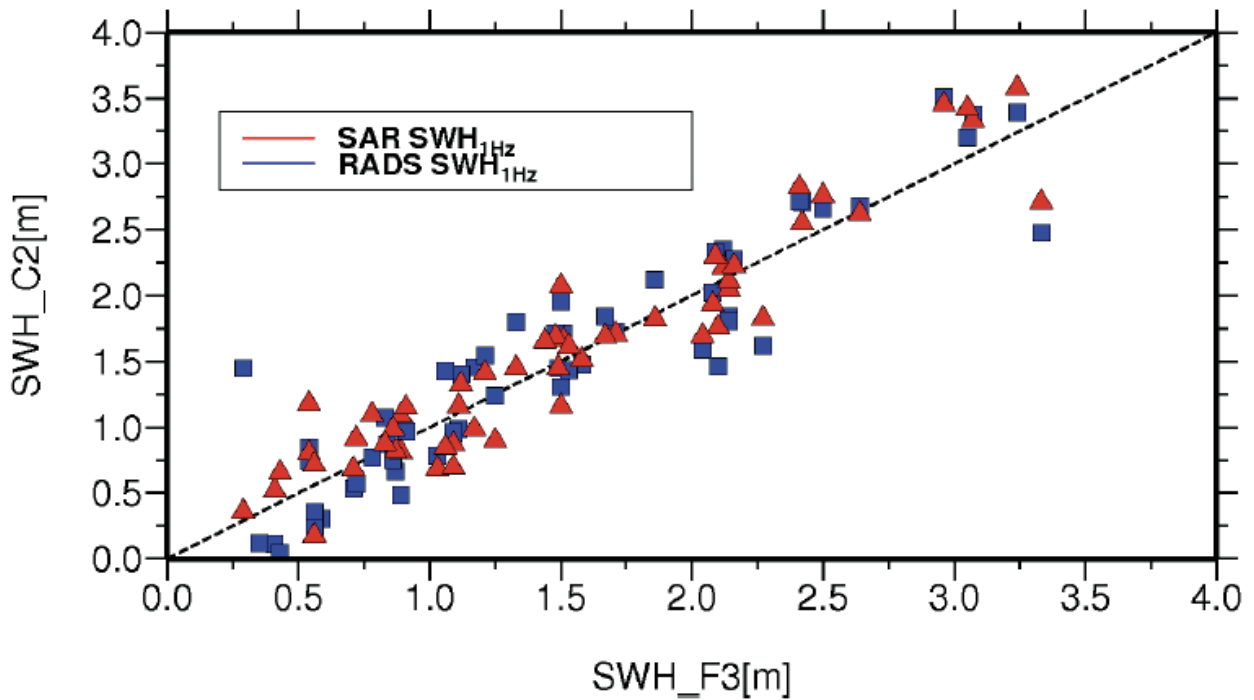
More recently, Fenoglio-Marc (2013) presented independent validation of Cryosat-2 SAR SWH against buoys in the German Bight (Figure 17). These analyses, based on Cryosat-2 SAR L1B



waveforms produced with the ESRIN L1B SAR processor retracked with the SAMOSA3 model (Dinardo *et al.*, 2012), confirmed that SAR mode retrieves unbiased values of SWH against buoys, even at low wave heights, when the production of SAR L1B waveforms is optimised for ocean (i.e. no Hamming filter).

Introduction Methods | **Results** | Conclusions

SWH comparison with In-situ FINO3



many SWHs are lower than 1 meter

(50 Km, 30 Minutes, 57 Points)



Dresden 12-14 March 2013

17

FIGURE 17: CRYOSAT-2 SAR RETRIEVED SIGNIFICANT WAVE HEIGHT AGAINST SWH MEASURED AT THE FINO3 PLATFORM IN THE GERMAN BIGHT (SOURCE: FENOGLIO-MARC, 2013)

APPENDIX B. SAR ALTIMETER WAVEFORMS AND RETRACKING MODELS

In altimetry (LRM or SAR mode) geophysical estimates of sea surface height, significant wave height and backscatter coefficient are obtained by fitting a theoretical waveform model dependent on the geophysical parameters to the measured waveforms.

For conventional pulse-limited altimeters, the theoretical model of reference for ocean type waveforms is the Brown model (Brown, 1977). This analytical formulation is derived from the double convolution of Flat Sea Surface Response (FSSR), the Radar Point Target Response (PTR) and the Probability Density Function (PDF) of surface elevation (Barrick, 1972; Barrick & Lipa, 1985). The first analytical derivation of the double convolution was performed by Brown (1977), but other authors included simplifications or modifications depending on the purpose.

An example of Brown fitting is shown in Figure 18. Note that other models have followed Brown to account for further observation parameters. For example, Hayne (1980) introduced higher order moments of the PDF and PTR terms, Rodriguez (1988) simplified the Brown model considering the pointing angle is less than 0.3° , Amarouche *et al.* (2003) introduced a second order term to account for higher mispointing angle up to 0.8° . The latter is used in Jason-1, Jason-2 and SARAL operational processing. Generally, the PTR is approximated by a Gaussian function to allow a complete analytical derivation of the model. In that case, look-up tables are necessary to correct for some sea state correlated biases (Thibaut *et al.*, 2004).

For SAR altimetry the shape of the backscattered waveforms over the ocean appear peakier than in conventional altimetry, thus Brown nor later derivations of it, are any longer suitable for fitting SAR mode altimetry data (see Figure 18b).

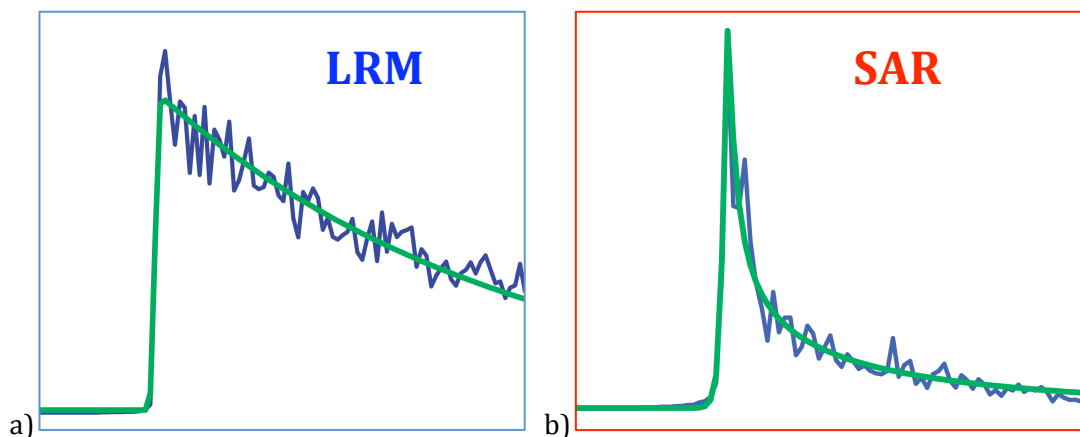


FIGURE 18: TYPICAL OCEAN TYPE ALTIMETER WAVEFORMS IN LOW-RATE MODE (LRM; LEFT) AND SAR MODE (SAR; RIGHT) FITTED WITH THE BROWN OCEAN MODEL AND THE SAMOSA SAR ALTIMETER MODEL RESPECTIVELY.

As in conventional altimetry, the mean power of a SAR altimeter echo over the ocean is derived from the convolution of three terms: the surface impulse response (P_{surf}), the system point target response (PTR) and the sea surface height probability density function (PDF_{sea}).

$$P(f, t) \propto \sigma^0 G^2(f, t) P_{surf}(f, t) * PTR(f, t) * PDF_{sea} \quad \text{Eq. 1}$$

where σ^0 is the backscatter coefficient and G the antenna gain pattern.

Hence, in SAR altimetry, the reflected power is a two-dimensional function of time (delay) and distance along-track from nadir (Doppler frequency). The model depend on various ocean geophysical parameters of interest (range, significant wave height and backscatter coefficient from which one derives wind speed) and other parameters linked to geometry, satellite orbit parameters, platform attitude, etc... From this model, the stack of echoes staring at a particular ground cell is built and incoherently summed to form the one-dimensional SAR multi-looked waveform that is used to fit measured waveforms. An example of a stack is shown in Figure 19.

In the following sections, we outline various solutions that have been proposed to compute Eq. 1.

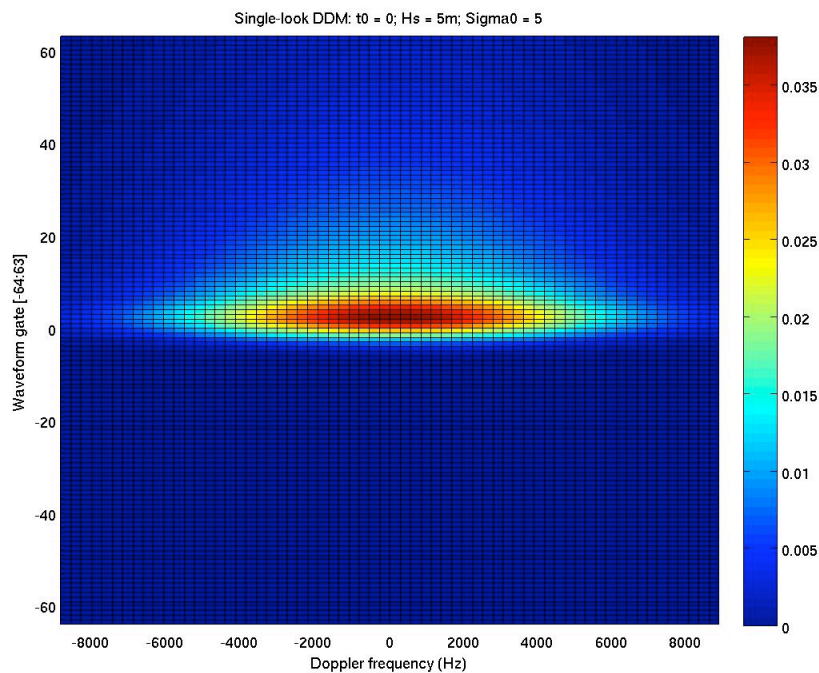


FIGURE 19: EXAMPLE OF A SAR ALTIMETER TWO-DIMENSIONAL DELAY-DOPPLER MAP OR STACK, REPRESENTING THE DISTRIBUTION OF RECEIVED POWER AS A FUNCTION OF DELAY (TIME) AND DOPPLER FREQUENCY (DISTANCE FROM NADIR ALONG-TRACK WITHIN THE ANTENNA BEAM). THIS EXAMPLE CORRESPONDS TO AN EPOCH = 0, SIGNIFICANT WAVE HEIGHT = 5 METRES, AND BACKSCATTER COEFFICIENT = 5, WITH PLATFORM MISPOINTING ALONG-TRACK AND ACROSS-TRACK BOTH EQUAL TO 0.



B.1. NUMERICAL SAR WAVEFORM MODELS

In this scheme, the triple convolution in Eq. 1 is computed numerically to provide an exact solution for the SAR waveform. This is the method adopted by TAS (Phalippou & Enjolras, 2007; Phalippou & Demeestere, 2011) and by CNES (Boy *et al.*, 2012). In principle, the method offers an exact solution to the problem by making it possible to account for complex forms of the various terms, for example the antenna gain pattern or the PTR, without the need for approximations.

In practice, the method is computationally expensive since the convolution has to be computed for a wide range of geophysical, geometrical and orbital parameters (satellite height and velocity, mispointing angles, etc.) to build a look-up table (LUT) of waveforms that accounts for all these effects on the waveforms. In practice therefore, for the sake of computational expediency, approximations are sometimes made e.g. by assuming a circular antenna pattern instead of the slightly elliptical one used for Cryosat-2, or by considering constant platform mispointing angles along the orbit. However, once the LUT has been computed, its use in operational schemes makes for efficient retrieval.

B.2. SEMI-ANALYTICAL SAR WAVEFORM MODELS

Wingham *et al.* (2004) proposed a semi-analytical solution to Eq. 1. The model accounts for the slight ellipticity of the Cryosat-2 antenna beam and shows explicit dependence of the SAR waveforms on platform mispointing angles. The method still depends on the prior computation of look-up tables with sufficiently fine parameter resolution to calculate some terms of the model (Giles *et al.*, 2012).

Halimi *et al.* (2012) developed a semi-analytical model where the FSSR function is modeled using an analytical formula and the double convolution with the ocean Power Density Function and Range and azimuth Impulse Responses is performed numerically. The model accounts for 5-parameters, including mispointing angles in across and along-track directions.

Within the ESA-funded SAMOSA⁴ project, three models were developed to compute the two-dimensional delay-Doppler maps of scattered power in SAR mode, from which SAR mode altimeter waveforms can be derived. The three models correspond to different assumptions and different levels of complexity and are known as SAMOSA1 (Martin-Puig *et al.*, 2008), SAMOSA2 (Ray *et al.*, 2013), and SAMOSA3 (Gommenginger *et al.*, 2012a). Fully analytical forms were obtained for SAMOSA1 and SAMOSA3 (see next section). SAMOSA2 is semi-analytical but provides the most complete solution, accounting for curvature effect along and across track, the ellipticity of the antenna pattern, non-Gaussian ocean surface statistics, radial velocity effects and mispointing effects along and across track. However, its semi-analytical form makes it computationally slow compared to fully analytical models.

B.3. FULLY-ANALYTICAL PHYSICALLY-BASED SAR WAVEFORM MODELS

The SAMOSA1 model is a fully analytical form developed under the assumptions of Gaussian ocean surface statistics, no curvature effect across-track, no mispointing across-track and circular antenna

⁴ <http://www.satoc.eu/projects/samosa/>

pattern. SAMOSA3 is also fully analytical, but being a simplification of SAMOSA2 (see above) for Gaussian ocean surface statistics, otherwise benefits from all the other advantages of SAMOSA2. For example, SAMOSA3 captures the important sensitivity of the shape of the SAR waveforms to mispointing angle across-track (roll angle) as shown in Figure 20.

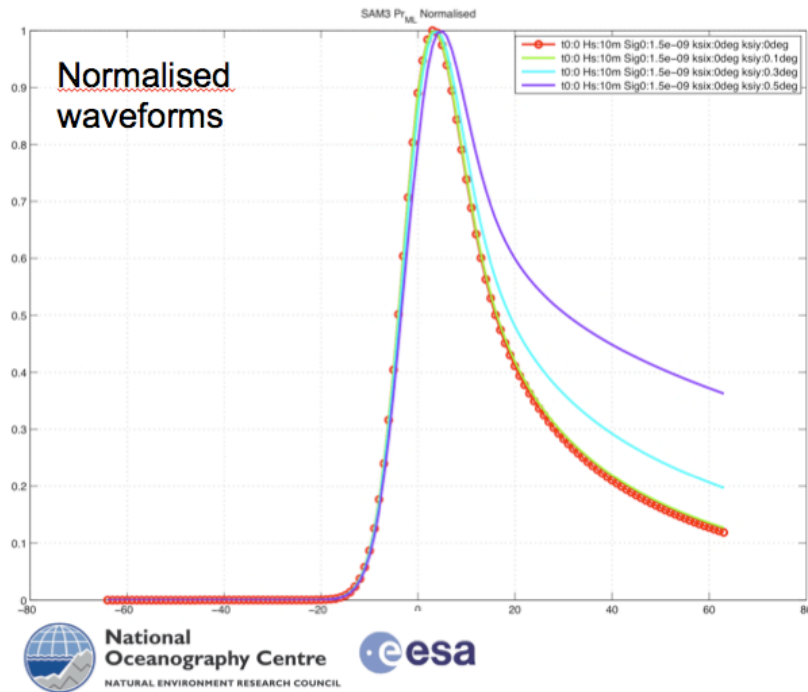


FIGURE 20: SAR ALTIMETER WAVEFORMS COMPUTED WITH THE SAMOSA3 MODEL FOR SIGNIFICANT WAVE HEIGHT = 10 METERS, ALONG-TRACK MISPOINTING = 0 DEGREES AND ACROSS-TRACK MISPOINTING = 0 (RED), 0.1 (GREEN), 0.3 (CYAN) AND 0.5 (PURPLE) DEGREES (SOURCE: GOMMENGINGER *ET AL.*, 2011)

The SAMOSA3 model has been validated extensively against simulated and real Cryosat-2 data and has been selected as the SAR ocean retracker model for the operational processing chain of the Sentinel-3 STM mission.

B.4. EMPIRICAL SAR WAVEFORM MODELS

An empirical fully-analytical model has been proposed by Sandwell *et al.* (2011) for the purpose of retracking Cryosat-2 SAR waveforms for improved marine gravity. While the formulation is indeed simple, it is not clear how/whether the empirical model captures the effect of the asymmetric antenna pattern and the influence of mispointing. Since the 20Hz range noise obtained for Cryosat-2 SAR data with this empirical model is larger than that observed by other groups, the authors concluded that this “fully-analytic retracking model is suboptimal” (Sandwell *et al.*, 2011).



APPENDIX C. OPEN ISSUES

Three open issues about SAR altimetry merit discussion, since they are still under investigation.

Note that, with the adoption of SAR interleaved mode on Jason-CS, these issues would simply disappear as potential concerns, since the SAR-mode data can then be compared directly with LRM data over the same surface and viewing geometry. Thus, SAR interleaved would deliver the advantages of SAR altimetry while ensuring that the data are at least as good as conventional altimeter products under all conditions.

C.1. SENSITIVITY TO PLATFORM MISPOINTING

As shown in Figure 20, SAR altimeter waveforms show some dependence on platform mispointing, in particular across-track mispointing (roll angle), which affects the shape of the waveform in a similar way to an increase in significant wave height. Validation of Cryosat-2 SAR SWH against buoys (Section A5) confirms the sensitivity of SAR SWH to platform mispointing, where an error in mispointing can result in significant bias in SWH. The mispointing used as input to the SAR retracker must therefore be as accurate as possible.

For Cryosat-2, it has been shown that the platform mispointing angles derived from the star-trackers are slightly biased. Several groups have developed methods to estimate the mispointing bias, which needs to be applied to the measured mispointing before being used as input to the SAR retracker. Using both SARIn and SAR calibration methods, Galin & Wingham (2013) estimate the roll and pitch biases for Cryosat-2 to be 0.1062 degrees and 0.052 degrees respectively. These differ from estimates by other investigators with a different method (e.g. W. Smith, R. Scharroo, F. Boy), who report roll and pitch biases of 0.0848 degrees and 0.0962 degrees. At this stage, the origin of the discrepancy is not understood. Similarly, the sensitivity of retrieved range to errors in mispointing remains to be fully investigated.

C.2. SSB IN SAR MODE

At the time of writing, there is no sea state bias model for SAR mode altimetry. Given the marked differences between SAR and LRM echoes and scattering, there is no reason at this stage to assume that LRM SSB models can be applied to SAR data.

There are two main methods to derive sea state bias models: the direct method (based on anomalies from the mean sea surface) and the crossover method (based on anomalies at crossovers). Both methods need large amounts of data over a wide range of wind and wave conditions to populate the [σ_0 , SWH] grid from which a SSB model may be derived.

At present, this topic is still work in progress, as the amount of processed SAR SLA data remains small. Global SAR SLA from CNES CPP are the most likely way for progress to be made on this subject in the next few months and work is already underway. Early estimates, based on a small amount of SAR SLA data from CPP, suggest that the difference in SSB between SAR and LRM is of the order of 0.5% of SWH (Labroue *et al.*, 2013).

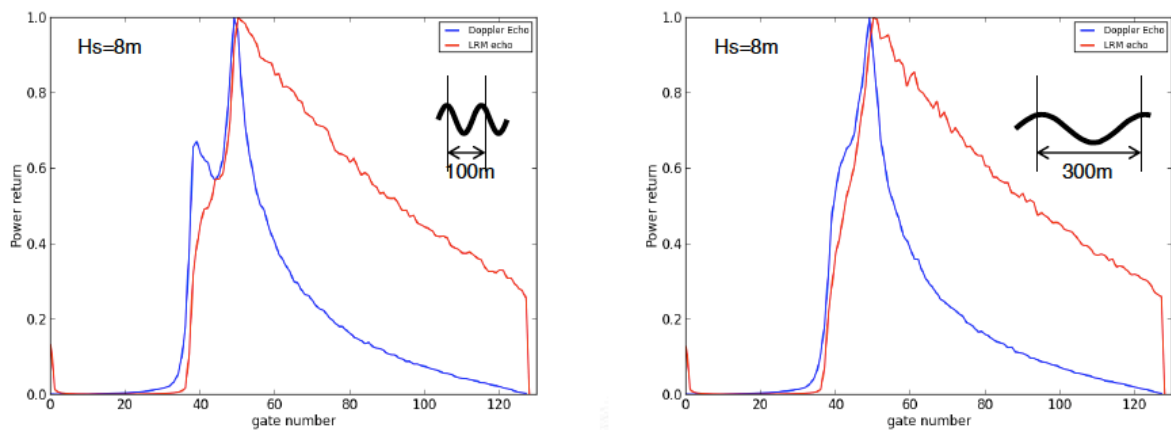
Ultimately however, even once the full Cryosat-2 SAR dataset has been processed, it is possible that the limited extent of SAR regions in the Cryosat-2 mode mask will not provide sufficient data to deliver a robust SAR SSB model, bearing in mind that non-geophysical factors important for SAR altimetry (orbit rate, mispointing angle) will also need to be accounted for as part of the development of the SAR SSB model.

C.3. EFFECT OF SWELL AND SWELL DIRECTION ON SAR MODE WAVEFORMS

With the effective along-track spatial resolution of ESA Cryosat-2 SAR mode data estimated at 450 metres (Scagliola, 2013), it has been suggested that SAR mode data may be sensitive to long swell waves, which may introduce possible biases in the SAR measured SSH (and perhaps also SWH).

The issue currently is being investigated by Moreau *et al.* (2013) and Gommenginger *et al.* (2013).

Based on the CNES/CLS end-to-end SAR Radar Simulator, Moreau *et al.* (2013) were able to produce simulated LRM and SAR waveforms for a variety of swell scenarios. Results suggest that SAR waveforms may become broader, or even double-peaked, in the presence of swell (Figure 21).



- Note that the front edge of the LRM waveforms is also modified by the swell (more impacted by short-wavelength swell)

FIGURE 21: SIMULATED LRM (RED) AND SAR (BLUE) WAVEFORMS FROM THE CNES/CLS SAR RADAR SIMULATOR FOR TWO SCENARIOS WITH SWH = 8 METRES AND SWELL WAVELENGTH IS (LEFT) 100 METRES AND (RIGHT) 300 METRES (SOURCE: MOREAU *ET AL.*, 2013)

Since the SAR waveform simulator makes it possible to produce simulated SAR waveforms for ocean surface scenarios with swell travelling in different directions, it is also possible to quantify the effect of swell direction. Early results indicate that the effects are present for both along-track and across-track travelling swell. Moreau *et al.* (2013) also reported evidence of double-peaked waveforms in Cryosat-2 CPP SAR waveforms in the central Pacific, where swell is frequent.



Using swell data from Envisat ASAR available through the Globwave project, Gommenginger *et al.* (2013) later confirmed that long swell leads to distorted or double-peaked Cryosat-2 SAR waveforms in the Pacific (Figure 22).

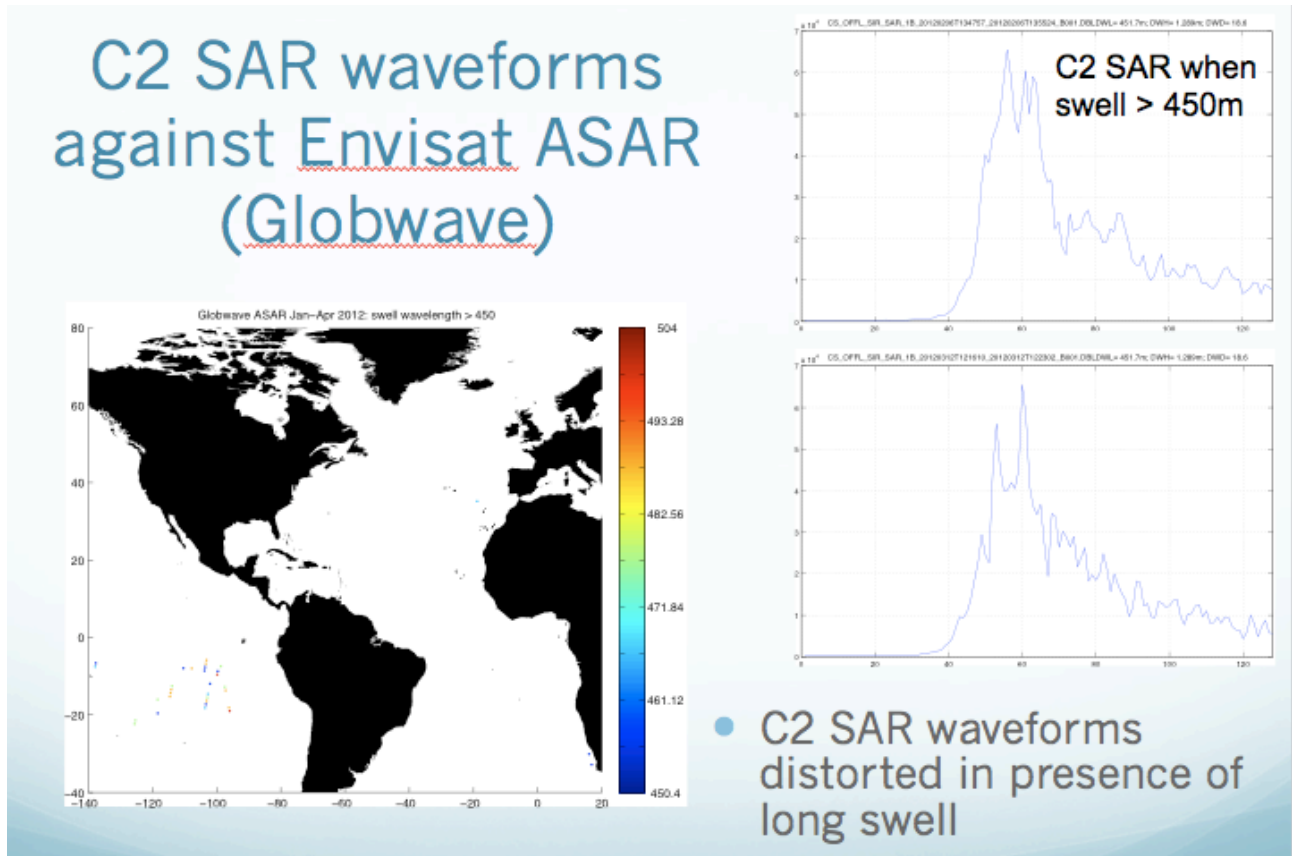


FIGURE 22: (RIGHT) DISTORTED CRYOSAT-2 SAR WAVEFORMS IN THE PACIFIC OCEAN IN THE PRESENCE OF LONG SWELL WAVES, WITH SWELL CONDITIONS ASCERTAINED WITH (LEFT) OCEAN WAVELENGTH ESTIMATES FROM ENVISAT ASAR DATA PROVIDED THROUGH GLOBWAVE (SOURCE: GOMMENGINGER *ET AL.*, 2013)



APPENDIX D: LRM AND SAR MODES: CLOSED BURST VS INTERLEAVED OPERATION

CryoSat-2 is the first radar altimeter to offer more than one operating mode from the same instrument. Its three modes are known as the Low Resolution Mode (LRM) which is essentially a conventional radar altimeter, the high-resolution mode which is the first time from Earth space that a radar altimeter uses synthetic aperture radar techniques (SAR mode), and the two-antenna cross-track interferometry (SARIn) mode. The latter is useful primarily over sloping ice sheets, and therefore is not being considered for an oceanographic altimetric mission such as Jason-CS.

In LRM the transmitted and received pulses are interleaved, which has been the case for all of the preceding missions outlined in section 3 above. The primary output product of a conventional radar altimeter is a set of so-called waveforms, each one of which is generated by averaging a sequence of the reflection histories of the time-varying response to each individual transmitted pulse. The classical product is the Brown waveform (Brown, 1977). More averaging leads to smoother waveforms, which is good. More averaging per unit time requires that the radar's PRF be larger. However, as discussed, there is an upper limit on PRF, because if it is too high, then more averaging no longer contributes to a smoother waveform. As a result, the pulse repetition frequency (PRF) employed by LRM radar altimeters typically is on the order of 2000 pulses per second (equivalently⁵, 2 kHz). The TOPEX PRF of 4 kHz is an important exception (Zieger *et al.*, 1991), explored below.

SAR mode operation adds new dimensions to the instrument, since the (partially) coherent processing breaks the received data by Doppler frequency selection into many parallel narrow neighbouring along-track beams, in combination with across-track cells that are resolved in the conventional pulse-limited manner (Raney, 1998). The corresponding theory is well understood.

In the SAR mode as designed for CryoSat-2 and Sentinel-3, bursts of 64 pulses are transmitted. This form of the SAR mode is known as closed burst operation (Raney, 1998) because, unlike an interleaved arrangement, there are no receptions that would follow each of the individual pulse transmissions. Instead, the reflections arrive back at the radar as a received burst after each transmitted burst has finished (Figure 23). The process repeats: transmitted bursts of pulses, each followed by received bursts of reflections. The alternative is an open burst architecture, in which receptions occur after each pulse, as is the case with an interleaved LRM radar. Thus, in addition to the PRF within each burst, closed burst architecture introduces two new parameters: *burst length* and *burst period*. These two parameters emerge as central characters in the issues surrounding the choice of SAR mode for implementation on Jason-CS.

⁵ Hertz is the standard unit name for "cycles per second", abbreviated "Hz".

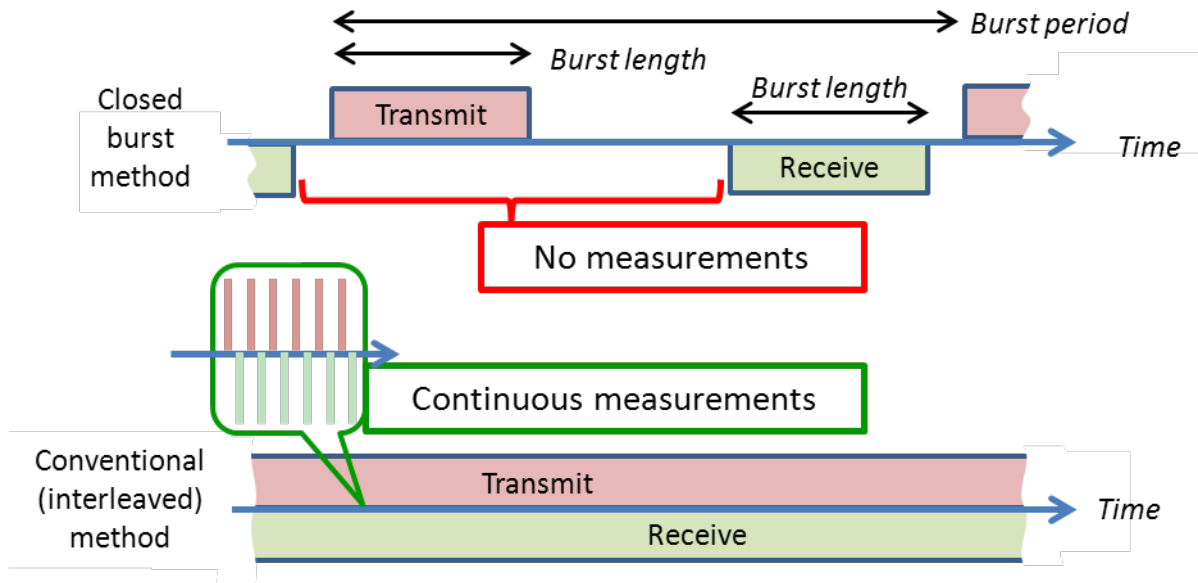


FIGURE 23: CHRONOGRAMS FOR THE CLOSED BURST MODE (UPPER) AND THE INTERLEAVED MODE (LOWER)

The PRF within each burst for a SAR mode must be much higher than an LRM mode requires. The CryoSat-2 PRF was chosen to be about 18 kHz, a value which assures that there are no Doppler ambiguities created⁶. However, it has been shown (Raney, 2010) that such a high PRF is not required for an altimeter viewing the ocean from directly above. A PRF on the order of 9 kHz would suffice, with adequate margins, which is low enough to allow space between transmitted pulses for open burst receptions.

Although CryoSat-2, as the first Earth-orbiting SAR mode radar altimeter, was implemented with a closed burst architecture, there is no technical reason why an open burst approach would not be acceptable. Indeed, TOPEX used an open burst strategy (Zieger *et al.*, 1991). Although its PRF was constant, it was not perfectly continuous. At periodic intervals the pulse sequence was retarded or advanced by small increments to compensate for the inevitable small changes in spacecraft altitude, so that the subsequent received data would always arrive between transmissions. It is an excellent example of the open burst approach, in which the successive transmission bursts are essentially abutting, the optimum situation for an interleaved altimeter. Its 4 kHz PRF is approximately half of that which would be required for an open burst SAR mode implementation.

The closed burst method, by definition, creates gaps between receptions during which the radar fails to make observations. For example in the CryoSat-2 case, the receiver is effectively “turned off”

⁶ The requirement to avoid Doppler ambiguities would apply if the radar were side-looking as is the case for an imaging SAR (for which the PRF must satisfy the Nyquist sampling rule with respect to the Doppler bandwidth of reflections within the antenna pattern), but it does not apply to the special case of a down-looking ocean-viewing radar altimeter.



about 70% of the time. Although the data collected by CryoSat are adequate for its mission, a 70% loss of data should be deemed intolerable for a Jason-class oceanographic mission.

The issue goes beyond an obvious compromise in data collection, and hence in data quality. A major and very reasonable interest in the radar altimeter community is to establish the performance of SAR altimetry against the standard of conventional altimetry. To enable quantitative comparisons, it would be ideal to obtain measurements by two altimeters, one in SAR mode and the other LRM, over the same oceanic surface, at the same time. Although awkward if not impossible to realize if relying only on two different spacecraft, there is in principal a relatively simple way to achieve the same result. The trick⁷ is to compare true LRM waveforms to those derived from SAR mode data (pseudo-LRM or P-LRM waveforms) when created from the same SAR mode data. Such experiments have been exercised on CryoSat-2 data over selected ocean sites. The results are good (Section A.2), in the sense that “similarity” can be achieved between the two kinds of waveforms. Predictions of improved measurements from the SAR-mode in comparison to LRM-based measurements have been verified.

There is an associated result that is of more general significance: it is impossible to generate “pseudo-LRM” (P-LRM) waveforms from closed-burst SAR-mode data that replicate waveforms (by which is meant two different waveforms that enjoy statistical equivalence) from the CryoSat-2 LRM mode under the same viewing and sea-state conditions. The scale of the discrepancy is captured by one parameter, the ratio ΔT of the receive burst length to the burst period (Figure 23). This number for any closed burst altimeter must be less than 0.5, and is equal to 0.33 in the case of CryoSat-2. As a consequence, the uncertainty in a measurement such as sea surface height (SSH) derived from the P-LRM data would be larger (thus poorer) than that obtained from the true LRM mode by the factor $(1/\Delta T)^{1/2}$, which is nearly a factor of 2 for CryoSat-2. The resulting P-LRM to LRM comparisons are sufficient to show that the SAR mode measurements are significantly superior to LRM-based measurements, but “similarity” falls short of quantifying how much “better” the SAR-mode based measurements might be.

This result has a direct bearing on Jason-CS, for which a major requirement is to guarantee continuity between measurements from Jason-CS and the 20-year heritage of measurements from earlier mission on the same orbit. That requirement cannot be satisfied if Jason-CS uses the closed-burst SAR mode. Further, Jason-CS is required to support continuity across platforms, so that its measurements may be quantitatively compared to LRM measurements from other altimeters at crossovers, for example. This requirement also cannot be met if Jason-CS uses only the closed burst architecture.

One might argue that if the value of the discrepancy is known, then it could be inverted and applied as a correction factor, with the intent to arrive at a meaningful comparison between the waveforms derived from closed-burst SAR mode, and the corresponding LRM waveforms from any source desired. Perhaps so, but that subterfuge at best would be far less convincing than a true comparison between constituents that should be statistically equivalent without application of correction factors. Such equivalency will be true if and only if Jason-CS adopts the interleaved mode for SAR altimetry.

⁷ The methods and results of this approach are reviewed in Appendix E.





APPENDIX E. TRANSFORMATION OF SAR-MODE DATA INTO PSEUDO-LRM WAVEFORMS

CryoSat-2 enables opportunities for quantitative comparisons of SAR-mode and conventional radar altimeter (LRM) mode measurements. The high-level strategy is to start with SAR-mode data over a specific site, and in parallel to transform those data into waveforms that are intended to replicate LRM products, hence LRM measurements. This strategy provides sets of measurements from two different kinds of radar that may be compared quantitatively. To this point there is general agreement. However, in practice, there are several pitfalls to be recognized and overcome when making the intended transformation.

The terminology in use by those working with Cryosat-2 includes “RDSAR” (SAR Reduction), a generic term for the process by which “pseudo-LRM” (or P-LRM) waveforms are generated from SAR-mode data.

E.1. REPLICATING LRM WAVEFORMS FROM SAR-MODE DATA

At the outset it must be noted that LRM waveforms from a conventional radar altimeter cannot be replicated from closed-burst SAR-mode data, as Cryosat-2 experience illustrates so clearly. The fundamental reason once seen is simple: closed-burst operation requires that the radar cannot collect data while it is transmitting groups (bursts) of pulses. As a result, at least half of the potential data collection time cannot be used, because the radar needs to “listen” for at least as long as it “talks”. (For CryoSat-2 the radar does not listen 70% of the time.) In contrast, data collected through an interleaved SAR mode can be processed to replicate conventional waveforms. That is because all potential data collection time is exploited, in particular, all of the small intervals between each of the transmitted pulses. These points are elaborated in context below.

E.1.1. CLASSICAL CONVENTIONAL BROWN-STYLE WAVEFORM

One reasonable objective of transforming SAR-mode data is to generate pseudo-LRM waveforms that in general conform to the well-known Brown model (Brown, 1977), and more specifically, that are virtually identical to the waveforms that would be produced by the CryoSat-2 LRM mode if observing the same sea conditions. A less demanding objective would be to generate pseudo-LRM waveforms that are “similar” to true LRM waveforms. The RDSAR-generated data generated from CryoSat-2’s closed burst modality are confined to the category of “similarity”.

This opening discussion is meant to explore the general issue. For that purpose, consider a notional Brown waveform that is comprised of five distinct regions, each of which have properties determined by applicable physics or processing choices.

The noise floor. Prior to arrival of each reflection from the illuminated surface, the receiver contributes its own constituents to the observed signal. The dominant constituent is additive noise, well modeled by the classical complex zero-mean Gaussian random process. Such noise always is statistically independent pulse to pulse for any pulse repetition frequency (PRF). The (additive) signal-to-noise ratio (SNR) is the usual applicable metric, which is a quantitative comparison of the



respective mean signal (S) and noise (N_0) powers. The standard deviation of the additive noise is proportional to $1/(\text{square root of})$, if n individual detected statistically independent waveforms are summed.

Speckle. Each individual echo produced by a radar altimeter consists of the complex (phase-dependent) sum of many individual backscattering constituents. At any given instant, their combinations randomly reinforce or cancel each other, resulting in a very ragged “noise-like” signature. Such a signature, known as *speckle* when seen following square-law detection, is normal behaviour for any coherent reflection from a random surface. The resulting random variations turn into uncertainty (quantified by standard deviations) in subsequent measurements, such as SSH, retrieved from waveforms.

Alert: Speckle is not noise, even though it may be perceived by a user as a nuisance, thence a “noise” in the generalized sense. Reference to speckle as “noise” is not correct, and is to be discouraged. The distinction is central to the RDSAR issue, because speckle is governed by physics that differ fundamentally from those of additive noise. Additive noise is reasonably well quantified by the signal-to-noise ratio (SNR) of the total signal. If the signal is stronger, the SNR is larger. Larger SNR is better. In contrast, speckle is multiplicative, always having (mean) values that are proportional to (mean) signal strength. If the signal is stronger, then the speckle will be stronger by the same factor. As a multiplicative nuisance, the speckle-to-signal ratio (SSR) is a constant, independent of mean (random) signal strength. The SSR is reduced in response to summing more waveforms that are statistically independent: $SSR = S/\sqrt{N}$, where N is the number of statistically independent samples of the signal averaged together. Smaller SSR is better. (Specular backscatter typically is not plagued by speckle, but that is a separate topic.)

The relative value of the speckle is determined by the correlation properties of the constituent signal components. The speckle properties of two sequential individual waveforms from an ocean-viewing radar altimeter will be correlated if the pulse repetition frequency (PRF) is too high. Adding together waveforms whose respective speckles are correlated does not reduce the standard deviation of the retrieved measurements. The threshold PRF (Walsh, 1982) is known as the Walsh upper bound⁸ on pulse repetition frequency, here denoted PRF_w . The consequence is that if m individual detected waveforms are summed, the standard deviation of the resulting speckle will be reduced by the square root of m only if $PRF \leq PRF_w$. For conventional altimeters operating under this constraint, in one second $m = PRF$. Summed post-detection waveforms from PRFs larger than PRF_w will produce reduced additive noise standard deviation, but will not yield further reduced standard deviation of the speckle nor reduced uncertainty of the retrieved measurements.

The trailing slope. The trailing portion of a Brown-style waveform is characterized by decreasing average power, which for a conventional radar altimeter is determined primarily by the antenna pattern’s weighting. The same characteristic is expected for pseudo-LRM waveforms. If two or more

⁸ Note that the Walsh PRF upper bound is a soft limit, with gradual changes in pulse-to-pulse correlation as PRF_w is approached. The limit increases with increasing significant wave height as explained in section B.2.3.



complex (pre-detection) waveforms are coherently summed, the trailing slope is increased, converging in the limit to a very peaky shape as more received pulses are combined coherently. Since the objective of RDSAR transformation is a Brown waveform, this fact dictates that the process of generating a pseudo-LRM waveform from an ensemble of SAR-mode waveforms cannot include coherent pulse-to-pulse summation in any form. Stated alternatively, this implies that generation of pseudo-LRM waveforms should be comprised of operations on real (post-detection) waveforms, for which the power domain (magnitude squared) is a sensible modality.

Waveform leading edge and principal inflections. Measurements of sea surface height and significant wave height are derived using the leading edge of the averaged waveform (time delay and slope, respectively) from the pseudo-LRM waveform, as is customary with true LRM waveforms. The details of these two inflection regions as expressed in the ensuing P-LRM waveforms depend on the way in which the SAR-mode data are used to generate them.

E.2 RDSAR OPTIONS (FIVE CASES)

E.2.1. INTERLEAVED PARADIGM (CASES 1 AND 2)

Case 1. Requirement: Replicate the LRM waveform in all significant regards. When the transmitted and received signals are interleaved, the radar is free to operate with essentially continuous transmitted pulse repetition. This creates a substantial advantage relative to the closed burst method used by Cryosat-2, because there is no large gap between groups of receptions. The higher PRF is retained for the SAR mode (coherent) processing, but may be decimated to feed a conventional (incoherent) waveform processor. Decimation should be used, keeping one received pulse out of each sequence of q pulses. The parameter q should be chosen such that the SAR-mode PRF is reduced post-decimation to that of a typical (or intended) LRM instrument. The result is a P-LRM waveform that has the same statistics as the intended true LRM waveform in both additive noise and speckle, and has the same response to larger SWH height as would the LRM waveform.

Case 2. Requirement: Replicate the LRM waveform without regard for SWH effects, and minimize the additive noise. This is the same as Case 1, but without decimation. In brief, to get SAR-mode waveforms and their associated data products, process all data coherently (group by group) followed by the necessary incoherent additions [Raney, 1998]. To get pseudo-LRM mode waveforms and their associated data products, process the same data incoherently in the usual (conventional) manner, square-law detecting each waveform, followed by summations [Zieger, 1991]. The result is a P-LRM waveform that does not have the identical speckle statistics as the intended LRM waveform, because its response to larger SWH differs from that of the intended LRM waveform. Likewise, the P-LRM will have smaller comparatively additive noise than the corresponding LRM waveform. The two waveforms will be “similar”, but not statistically equivalent.

Commentary. These two cases are directly applicable to future radar altimeters such as Jason-CS operating in an interleaved mode. In this special case there is no loss implied by a gap between bursts of received data, since there should be no such gap. Case 1 is the basis for simultaneous generation of LRM and SAR-mode waveforms from the same data set (Raney, 2013). Case 1 (decimation) illustrates the way in which an interleaved SAR-mode data set could be processed to produce results that should



be virtually identical to conventional (lower PRF) radar altimeters, which therefor would assure continuity across LRM/SAR-mode transition boundaries, continuity between contemporaneous comparisons of LRM and P-LRM data at cross-overs from different altimeters, for example, and for continuity with respect to the 20+ year heritage of measurements from the T/P orbit. Note that Case 2 (no decimation) should not be expected to produce statistically equivalent replicas of reference LRM waveforms. Instead, Case 2 will produce “better” results than would Case 1, because the additive noise floor would have smaller standard deviation, and the speckle standard deviation would improve in response to larger SWH. One could envisage a SAR-mode altimeter operating interleaved, from which the standard products would be waveforms in SAR mode and LRM according to Case 2 for routine operations, while selected SAR-mode data could be reprocessed according to Case 1 for calibration and continuity purposes.

E.2.2. CRYOSAT-2, CLOSED-BURST PARADIGM (CASES 3 – 5).

As previously noted (Raney, 2010), the closed burst method severely restricts the amount of averaging available for improving measurement precision, because the radar is not able to collect data for about 70% of the time. Implementation in an open burst or interleaved strategy would enable approximately 3.3 times the number of statistically independent looks available from CryoSat-2, since the interleaved mode is designed to take advantage of all potential listening time. The interleaved-to-closed-burst comparison may be captured by one simple parameter: ***fraction of listening time*** ΔT , where $\Delta T = 1$ for the interleaved mode, and $\Delta T = (\text{burst length})/(\text{burst period})$ for the closed burst mode. Shorter listening time increases the resulting measurement standard deviation by a factor of $(1/\Delta T)^{1/2}$. For CryoSat-2, $\Delta T = 0.3$, which leads to a larger measurement standard deviation by a factor of 1.8 for CryoSat-2 data products than would be the case if the radar were to operate such that transmissions and receptions were interleaved.

The same factor applies to the generation of P-LRM waveforms from closed burst SAR-mode data. Since burst mode operation demands that less data are collected during any given time interval, it follows that closed burst SAR mode data are not sufficient to be reprocessed such that the result would truly replicate a sequence of LRM waveforms, no matter how clever the RDSAR technique may be. Missing data lead to larger measurement uncertainty when compared to otherwise comparable LRM products. The best that one could hope for would be a larger standard deviation of the P-LRM product with respect to the true LRM product by $(1/\Delta T)^{1/2}$.

The following cases, based on Cryosat-2, illustrate the principal RDSAR options that would be supported by the closed burst method, using 1 Hz (one-second averaging) for the examples. None of them generate P-LRM waveforms that would be fully equivalent to the intended true LRM waveforms. This shortcoming is a direct consequence of the burst-mode paradigm.

Case 3. Requirement: Replicate an individual LRM waveform. (This was the method recommended by the SAMOSA project.) In this case, the speckle and additive noise standard deviations respectively of the pseudo-LRM waveforms must each match those of a true LRM waveform. Thus, there must be the same number of statistically independent (post-detection) waveforms added together as in the LRM case, 1970 per second. That requirement implies decimation; only one out of 9 received SAR-mode post-detection waveforms should be employed in the summation, which leads to 8 usable returns per



burst, and 246 bursts to accumulate 1970 returns. One significant implication is that about 3 seconds of SAR-mode data are needed to generate each one second of pseudo-LRM waveform. In this sense the result is not an exact replica, because, unlike the interleaved case, it takes about three times as much SAR-mode data to form each one-second pseudo-LRM waveform. The main consequence is, to generate a sequence of waveforms at 1 Hz, two-thirds of the SAR-mode data required for any given P-LRM waveform would have to be re-used for the first adjacent P-LRM waveform, and one-third would be used again as part of the needed SAR mode ensemble for the second adjacent P-LRM waveform. Thus, although the method should lead to the correct (additive noise and speckle) statistics across the P-LRM sequence, it also introduces additional waveform-to-waveform correlation, an undesirable feature. That correlation increases the standard deviation of the 1 Hz P-LRM waveforms by a factor of about $(1/\Delta T)^{1/2} = 1.8$ for CryoSat-2 data.

Case 4. Requirement: Approximate the LRM waveform without regard for the impact on additive noise. This is a relaxed form of Case 3, in that all of the post-detection SAR-mode waveforms are used in the summation. The impact of this strategy is to reduce the additive noise standard deviation relative to Case 3 by $9^{1/2} = 3$, a compromise that may be acceptable for certain applications. Note, as in Case 3, that about 3 seconds of SAR-mode data are required for each resulting one-second pseudo-LRM waveform. Hence it introduces waveform-to-waveform correlation in the same way as in Case 3. There are additional consequences. This approach also reduces the speckle standard deviation by a factor of $(PRF/PRF_W)^{1/2} \approx 0.9$ since the higher effective PRF in this method pushes the effective pseudo-LRM PRF to the Walsh limit. Further, this method naturally produces smaller speckle standard deviation in response to higher SWH, unlike the behaviour of the true LRM waveform whose PRF is below the low SWH value of the Walsh PRF limit.

Case 5. Requirement: Approximate the LRM waveform under the constraint that only one second of SAR-mode data are to be used for each one second of pseudo-LRM waveform, and without regard for the additive noise. This may be implemented simply by exercising Case 4 for only one second. The direct impact of this approach would be to generate pseudo-LRM waveforms that have larger speckle standard deviation than for the true LRM by a factor of about 1.5, and smaller additive noise standard deviation by a factor of about 1.7. Such waveforms would have the similar general appearance as true LRM waveforms, but following closer scrutiny would not have the correct additive noise nor speckle statistics at the 1-Hz or 20-Hz levels, nor would they have the correct response to higher SWH.

E.2.3. THE EFFECTS OF SWH ON PSEUDO-LRM WAVEFORMS

As implied above, larger significant wave height ($H_{1/3}$) has a direct impact on the effective pulse-limited diameter D_{PL} of the footprint of a conventional altimeter. Larger D_{PL} in turn implies a higher value for the Walsh upper bound on the number of available uncorrelated waveforms. The result is that the amount of averaging available (which is known as the Walsh limit for conventional (LRM) radars) increases with SWH, thus reducing the standard deviation of retrieved measurements.

These effects may be quantified. The Walsh upper bound is given by

$$PRF_{Walsh} = \frac{2K D_{PL}}{\lambda h}$$



where V is the spacecraft along-track velocity, λ is the radar's wavelength, and h is the mean altitude of the spacecraft above the Earth's surface. This equation is a more user-friendly form [Raney 2013] than usually is seen, but it may be derived directly from the classic equation [Walsh]. The effects of significant wave height reside inside the pulse-limited footprint diameter⁹ according to

$$D_{PL} = 2 \frac{\rho_{SWH}}{1 + \frac{h}{R_E}}$$

where ρ_{SWH} is the effective (single-pulse) range resolution of the radar when viewing the ocean's surface modulated by waves. The radar's intrinsic range resolution ρ meters is expanded by the surface waves into the larger effective resolution. (In this and the following discussion the minor effect of Earth curvature R_E is disregarded.) The original estimates of the impact of $H_{1/3}$ were in the form of

$$\rho_{SWH} = \rho + H_{1+3}$$

More sophisticated analyses (Sandwell & Smith, 2001) that account for a Gaussian distribution of backscattering elements over the entire surface wave profile arrive at SWH dependence in the form of

$$\rho_{SWH} = \rho^2 + a H_{1+3}^2 c^{\frac{1}{2}}$$

where the weighting constant a has a value on the order of 0.2. Using this expression, the general trends of footprint diameter D_{PL} and effective pulse length ρ_{SWH} from the T/P orbit (1334 km) are expressed graphically in.

Note, for a SAR-mode altimeter, that the along track resolution is essentially a constant, such as 300 m, regardless of SWH. Thus, for this example which applies directly to Jason-CS, the comparative advantage of SAR-mode operation over conventional altimetry is an improvement in along-track resolution of approximately a factor of 10 at mean 2-m SWH, and nearly a factor of 20 at mean 6-m SWH.

⁹ Note that this equation differs by a factor $\sqrt{2}$ with respect to expressions seen in much of the literature. That discrepancy is due to an error in a prime reference in which the transformation from pulse length τ seconds (compressed) to spatial pulse length ρ meters is given incorrectly by $\rho = c \tau$ (where c is the speed of light), rather than by the correct equivalence $\rho = c \tau / 2$.

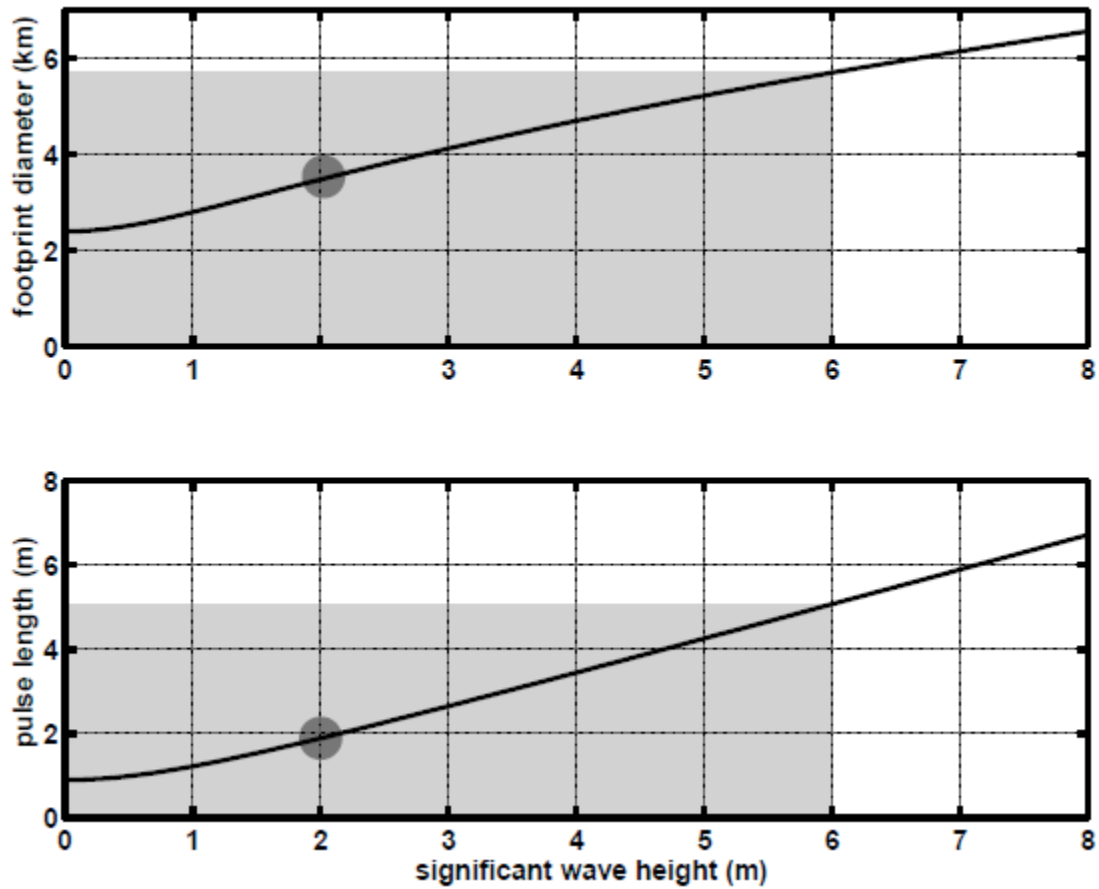


FIGURE 24: (LOWER) RETURN PULSE LENGTH IN METERS AS A FUNCTION OF SIGNIFICANT WAVE HEIGHT. (UPPER) DIAMETER OF THE RADAR PULSE ON THE OCEAN SURFACE AS A FUNCTION OF SIGNIFICANT WAVE HEIGHT. A TYPICAL SIGNIFICANT WAVE HEIGHT OF 2 M IS MARKED BY A LARGE GRAY DOT (SOURCE: SANDWELL & SMITH, 2001)



9. LIST OF ACRONYMS

2kR-LLC	A privately held company for non-commercial research based in Annapolis, MD, USA
aka	also known as
CLS	Collecte Localisation Satellites
CPP	Cryosat-2 Prototype Product (produced by CNES)
LRM	Low resolution mode (aka pulse-limited, or conventional)
P-LRM	Pseudo-LRM (aka Reduced SAR)
PRF	Pulse repetition frequency
SAR	Synthetic Aperture Radar
SLA	Sea Level Anomaly
SSB	Sea state bias
SWH	Significant Wave Height (aka as H_s or $H_{1/3}$)
TAS	Thales Alenia Space



10. REFERENCES

- Amarouche, L., P. Thibaut, O. Z. Zanife, J.-P. Dumont, N. Steunou, & P. Vincent, 2003: Improving the Jason-1 ground retracking to cope with attitude effects. *Marine Geodesy, Special Issue on Jason-1 Calibration/Validation, Part 2*.
- Barbarossa, S.G. Picardi, 1990: The synthetic aperture concept applied to altimetry: Surface and sub-surface imaging. Proceedings of the consultative meeting on imaging altimeter requirements and techniques, C.G.Rapley, H.D. Griffiths and P.A.M. Berry, Eds., 30 May - 1 June 1990, Dorking, UK., Mullard Space Science Laboratory Report MSSSL/RSG90.01.
- Barrick, D. E., 1972: Remote Sensing of the Sea State by Radar. In *"Remote Sensing of the Troposphere"* (V. E. Derr, ed.), Ch. 12, U. S. Govt. Printing Office, Washington, D.C.
- Barrick, D. E.B. J. Lipa, 1985: Analysis and interpretation of Altimeter sea echo. *Adv. Geophys.*, 27(3), 61-100.
- Boy, F., J.-D. Desjonqueres, & N. Picot, 2011: Cryosat Processing Prototype (CPP): CryoSat LRM, TRK and SAR processing. *Oral presented at the Ocean Surface Topography Science Team 2011, San Diego, July 2011, Available from: <http://www.avisooceanobs.com/?id=1692>.*
- Boy, F., J.-D. Desjonqueres, N. Picot, T. Moreau, S. Labroue, J.-C. Poisson, & P. Thibaut, 2012: Cryosat Processing Prototype: LRM and SAR processing on CNES side. *Ocean Surface Topography Science Team 2012, Venice, 27-28 Sept 2012, Available from: <http://www.avisooceanobs.com/en/courses/sci-teams/ostst-2012.html>.*
- Brown, G. S., 1977: The average impulse response of a rough surface and its applications. *IEEE Antennas and Propagation*, 25, 67-74.
- Cotton, D., M. Naeije, M.-P. Clarizia, O. Andersen, M. Cancet, A. Egido, J. Fernandes, C. Gommenginger, S. Labroue, M. Roca, J. Benveniste, N. Picot, & S. Dinardo, 2013: CP40 - Cryosat Plus for Oceans: An ESA STSE project, supported by CNES. *Cryosat Third User Workshop, Dresden, 12-14 March 2013*.
- Dinardo, S., B. Lucas, & J. Benveniste 2011: SAR Altimetry in Coastal Zone: Performances, Limits, Perspectives. *Fifth Coastal Altimetry Workshop, San Diego, 16-18 October 2011, Available from: <http://www.coastalt.eu/sandiegoworkshop11>.*
- Dinardo, S., B. Lucas, & J. Benveniste 2012: Echo Contamination in SAR Mode in coastal zone and calm waters. *Sixth Coastal Altimetry Workshop, Riva del Garda, 20-21 September 2012*.
- Dinardo, S.L. Fenoglio-Marc, 2013: Validation of CryoSat-2 in SAR mode in the German Bight. *Ocean SAR altimetry expert group meeting, National Oceanography Centre-Southampton, UK, 26-27 June 2013*.
- Fenoglio-Marc, L., 2013: A Validation Exercise for CRYOSAT-2 in SAR Mode in the German Bight Area. *Cryosat Third User Workshop, Dresden, 12-14 March 2013*.
- Ford, P. G.G. H. Pettengill, 1992: Venus topography and kilometer-scale slopes. *Journal of Geophysical Research: Planets*, 97(E8), 13103-13114.
- Fu, L.-L.A. Cazenave, 2001: *Satellite Altimetry and the Earth Sciences*. Academic Press



Galín, N.D. J. Wingham, 2013: Estimating Pitch Angle of CryoSat-2 using the Power Distribution of the Synthetic Aperture, Ocean SAR altimetry expert group meeting, National Oceanography Centre-Southampton, UK, 26-27 June 2013.

Giles, K., D. J. Wingham, N. Galín, R. Cullen, & W. Smith, 2012: Precise estimates of ocean surface parameters from Cryosat. *Ocean Surface Topography Science Team 2012*, Venice, 27-28 Sept 2012, Available from: <http://www.avisooceanobs.com/en/courses/sci-teams/ostst-2012.html>.

Gommenginger, C., C. Martin-Puig, S. Dinardo, D. Cotton, M. Srokosz, & J. Benveniste 2011: Improved altimetric accuracy of SAR altimeters over ocean: Observational evidence from Cryosat-2 SAR and Jason-2. *Ocean Surface Topography Science Team 2011*, San Diego, 19-21 Oct 2011, <http://www.avisooceanobs.com/en/courses/sci-teams/ostst-2011.html>.

Gommenginger, C., C. Martin-Puig, M. Srokosz, M. Caparrini, S. Dinardo, & B. Lucas, 2012a: Detailed Processing Model of the Sentinel-3 SRAL SAR altimeter ocean waveform retracker. SAMOSA3 WP2300 technical Note, ESRIN Contract No. 20698/07/I-LG "Development of SAR Altimetry Mode Studies and Applications over Ocean, Coastal Zones and Inland Water", Version 2.1.0, 16 March 2012, 75 pages

Gommenginger, C., P. Cipollini, D. Cotton, S. Dinardo, & J. Benveniste 2012b: Finer, Better, Closer: Advanced capabilities of SAR altimetry in the open ocean and the coastal zone. *Ocean Surface Topography Science Team 2012*, Venice, 27-28 Sept 2012, Available from: <http://www.avisooceanobs.com/en/courses/sci-teams/ostst-2012.html>.

Gommenginger, C. P., C. Martin-Puig, S. Dinardo, D. Cotton, & J. Benveniste, 2012: Improved altimetric performance with Cryosat-2 SAR mode over the open ocean and the coastal zone. *General Assembly of the European Geophysical Union (EGU 2012)*, Vienna, 22 - 27 April 2012.

Gommenginger, C. P., P. Cipollini, H. M. Snaith, L. West, & M. Passaro, 2013: SAR altimetry over the open and coastal ocean: status and open issues. *Ocean SAR altimetry expert group meeting, National Oceanography Centre-Southampton, UK, 26-27 June 2013*.

Hartl, P.Y. H. Kim, 1990: Multi-mode scanning radar altimeter (MSRA) with synthetic aperture. Proceedings of the consultative meeting on imaging altimeter requirements and techniques, C.G.Rapley, H.D. Griffiths and P.A.M. Berry, Eds., 30 May - 1 June 1990, Dorking, UK., Mullard Space Science Laboratory Report MSSL/RSG90.01.

Hayne, G. S., 1980: Radar altimeter mean return waveforms from near-normal incidence ocean surface scattering. *IEEE Antennas and Propagation*, AP-28(5), 687-692.

Jensen, J. R.R. K. Raney, 1998: Delay/Doppler Radar Altimeter: Better Measurement Precision. *Geoscience and Remote Sensing Symposium Proceedings, IGARSS '98, IEEE International, Volume 4, pp. 2011-2013*.

Labroue, S., T. Moreau, M. Raynal, F. Boy, N. Picot, & T. Parrinello, 2013: Quality Assessment of Cryosat-2 LRM & SAR over Ocean. *Cryosat Third User Workshop*, Dresden, 12-14 March 2013.

MacArthur, J. L., 1976: Design of the Seasat-A radar altimeter. *Oceans*, 8, 222-229.

MacArthur, J. L., C. C. Kilgus, C. A. Twigg, & P. V. K. Brown, 1989: Evolution of the satellite radar altimeter. *Johns Hopkins APL Technical Digest*, 10(4), 405-413.



Martin-Puig, C., J. Marquez, G. Ruffini, R. K. Raney, & J. Benveniste 2008: SAR Altimetry applications over water. *Proceedings of the ESA SeaSAR workshop, Frascati, Italy, January 2008*.

Martin-Puig, C., J. Marquez, & C. P. Gommenginger, 2010: CryoSat-2: from SAR FBR to LRM for quantitative precision comparison over identical sea state. *Proceedings of the ESA Living Planet Symposium, Bergen, Norway, September 2010*.

Moreau, T., S. Labroue, P. Thibaut, L. Amarouche, F. Boy, & N. Picot, 2013: Sensitivity of SAR Mode Altimeter to Swell Effect. *Cryosat Third User Workshop, Dresden, 12-14 March 2013*.

Phalippou, L.V. Enjolras, 2007: Re-tracking of SAR altimeter ocean power-waveforms and related accuracies of the retrieved sea surface height, significant wave height and wind speed. *Igarss: 2007 IEEE International Geoscience and Remote Sensing Symposium, Vols 1-12, 3533-3536*.

Phalippou, L.F. Demeestere, 2011: Optimal retracking of SAR altimeter echoes over open ocean: Theory versus results from SIRAL2 data. *Ocean Surface Topography Science Team 2011, San Diego, 19-21 Oct 2011*, <http://www.aviso.oceanobs.com/en/courses/sci-teams/ostst-2011.html>.

Phalippou, L., E. Caubet, F. Demeestere, J. Richard, L. Rys, M. Deschaux-Beaume, R. Francis, & R. Cullen, 2012: Reaching sub-centimeter range noise on Jason-CS with the Poseidon-4 continuous SAR interleaved mode. *Ocean Surface Topography Science Team 2012, Venice, 27-28 Sept 2012*, Available from: <http://www.aviso.oceanobs.com/en/courses/sci-teams/ostst-2012.html>.

Raney, R. K., 1998: The Delay/Doppler Radar Altimeter. *IEEE Trans. Geoscience and Remote Sensing*, 36 (5), 1578-1588.

Raney, R. K.J. R. Jensen, 2000: D2P project: Test campaign results. <http://fermi.jhuapl.edu/d2p/>.

Raney, R. K.C. J. Leuschen, 2002: LaRA-2002 Post-Flight Report SRO-02-13 (No. SRO-02-13). Laurel, Maryland: Johns Hopkins University APL; Raney, R. K., & Leuschen, C. (2003). LaRA/CryoVEx 2003 - Post-Flight Report (SRO-03M-29): Johns Hopkins University APL

Raney, R. K., 2005: *Radar Altimetry*. In K. Chang (Ed.), *Encyclopedia of RF and Microwave Engineering*, Vol. 5, pp. 3989-4005, Hoboken, NJ: John Wiley & Sons, Inc.

Raney, R. K., 2008: *Space-Based Remote Sensing Radars, Chapter 18*, In M. Skolnik (Ed.), *The Radar Handbook, 3rd Edition: McGraw-Hill*.

Raney, R. K., 2010: CryoSat SAR-Mode Looks Revisited. *ESA Living Planet Symposium, Bergen, Norway*.

Raney, R. K., 2013: Maximizing the intrinsic precision of radar altimetric measurements. *IEEE Geoscience and Remote Sensing Letters*, 10, 1171-1174.

Ray, C., C. Martin-Puig, M.-P. Clarizia, G. Ruffini, S. Dinardo, C. Gommenginger, & J. Benveniste 2013: SAR Altimeter Backscattered Waveform Model. *IEEE Transactions on Geoscience and Remote Sensing (sub judice)*.

Rodriguez, E., 1988: Altimetry for non-Gaussian oceans : Height biases and estimation of parameters. *J. Geophys. Res.*, 93, 14,107-114,120.



Sandwell, D. T.W. Smith, 2001: Chapter 12, Bathymetric estimation. In L.-L. Fu & A. Cazenave (Eds.), *Satellite Altimetry and the Earth Sciences: Academic Press*.

Sandwell, D. T., E. Garcia, & W. H. F. Smith, 2011: Improved Marine Gravity from Cryosat and Jason-1. *Ocean Surface Topography Science Team 2011*, San Diego, 19-21 Oct 2011, <http://www.aviso.oceanobs.com/en/courses/sci-teams/ostst-2011.html>.

Scagliola, M., 2013: Measuring the Effective Along-Track Resolution of CryoSat. *Cryosat Third User Workshop*, Dresden, 12-14 March 2013.

Scharroo, R., W. H. F. Smith, J. Lillibridge, & E. Leuliette, 2012: Global Cal/Val of Cryosat-2 LRM and SAR data over oceans. *Ocean Surface Topography Science Team 2012*, Venice, 27-28 Sept 2012, Available from: <http://www.aviso.oceanobs.com/en/courses/sci-teams/ostst-2012.html>.

Scharroo, R., W. H. F. Smith, E. Leuliette, & Lillibridge, 2013: The Performance of CryoSat as an Ocean Altimeter. *Cryosat Third User Workshop*, Dresden, 12-14 March 2013.

Thibaut, P., L. Amarouche, O. Z. Zanife, N. Steunou, P. Vincent, & P. Raizonville, 2004: Jason-1 altimeter ground processing look-up correction tables. *Marine Geodesy, Special Issue on Jason-1 Calibration/Validation, Part 3*.

Walsh, E. J., 1982: Pulse-to-pulse correlation in satellite radar altimetry. *Radio Science*, 17(4), 786-800.

Wingham, D. J., L. Phalippou, C. Mavrocordatos, & D. Wallis, 2004: The Mean Echo and Echo Cross Product From a Beamforming Interferometric Altimeter and Their Application to Elevation Measurement. *IEEE Transactions on Geoscience and Remote Sensing*, 42, 2305-2323.

Zieger, A. R., D. W. Hancock, G. S. Hayne, & C. L. Purdy, 1991: NASA radar altimeter for the TOPEX/Poseidon project. *Proceedings of the IEEE*, 79(6), 810-826.